Patterns and drivers of carbohydrate budgets in ice algal assemblages from first year Arctic sea ice

Shazia N. Aslam,[1] Christine Michel,[2] Andrea Niemi,[2] Graham J. C. Underwood*[1]
[1]School of Biological Sciences, University of Essex, Colchester, Essex, United Kingdom
[2]Fisheries and Oceans Canada, Freshwater Institute, Winnipeg, Manitoba, Canada

Abstract

Ongoing changes in sea ice distribution will have major implications for the ecology of the Arctic Ocean. First year ice (FYI) supports abundant ice-algae communities that produce dissolved and particulate carbohydrates, including extracellular polymeric substances (EPS), which are significant carbon sources, influence ice formation and microbial survival within sea ice, and water column carbon cycling following ice melt. Key drivers of the distribution and composition of these carbohydrates are poorly characterised. Carbohydrates and chlorophyll *a* concentrations were linearly related in springtime bottom FYI at 36 sites in the Canadian Archipelago region, with high levels of spatial heterogeneity. Nanoeukaryote cell density and phosphate concentration were strong drivers of total and dissolved carbohydrate and uronic acid concentrations. Particulate carbohydrates were strongly related to total bacterial abundance. Dissolved carbohydrates contributed 77% of total carbohydrate: the most abundant (51%) size fraction being dissolved carbohydrates < 8 kDa in size, with dissolved EPS contributing 7% to total carbohydrate. Carbohydrate fractions differed in monosaccharide profiles; dissolved components being glucose rich; particulate EPS containing more mannose, xylose, fucose and arabinose. These profiles corresponded to those of cultured sea-ice diatoms. Microbial abundance, silicate, nitrate and phosphate concentration and ice thickness were important environmental drivers, with thicker ice containing relatively more particulate EPS, with thinner ice containing high amounts of glucose-rich smaller-sized carbohydrate moieties. Changes in ice characteristics will alter the relative balance of labile and refractory carbohydrates generated within bottom ice layers, with implications for food webs and carbon turnover in the warming Arctic Ocean.

The Arctic Ocean only accounts for 1.4% of the total ocean volume, but contributes between 5% and 14% of the global balance of CO_2 sinks and sources (Bates and Mathis 2009). The Arctic is undergoing accelerated warming, twice as fast as the global average (Cohen et al. 2014), with significant changes in the areal extent, thickness and age profile of Arctic sea ice (Polyakov et al. 2012; Stroeve et al. 2012; Swart et al. 2015). The physical presence of ice and the productivity of ice-associated algae, support significant components of the marine polar food web (Carmack and Wassman 2006; Hop et al. 2006) such that the shift from thick multiyear to thinner first year ice (Stroeve et al. 2014; Swart et al. 2015)

will cause significant alterations in the ecology and biogeochemistry of the Arctic Ocean and its associated shelf seas (Clark et al. 2013; Vancoppenolle et al. 2013). Abundant autotrophic and heterotrophic microbiological communities, associated with high concentrations of dissolved (DOM) and particulate organic matter (POM), grow in sea ice, especially near the ice-water interface of first year ice (FYI) where freezing seawater forms a semi-solid matrix permeated by millimetre to submillimetre pores and channels (Thomas et al. 2010; Ewert and Deming 2013; Vancoppenolle et al. 2013). Ice-algal productivity makes a significant contribution to Arctic Ocean annual primary production, and is seasonally more significant during the spring-summer transition from full ice cover to open water, (Vancoppenolle et al. 2013; Fernández-Méndez et al. 2015).

Some DOM in sea ice originates from allochthonous organic material incorporated into ice during ice formation, but when DOM concentrations are high, this is primarily caused by autochthonous material produced via algal and microbial activity (Stedmon et al. 2007; Thomas et al. 2010). DOM in ice

---

includes a diverse spectrum of high and low molecular weight compounds with a wide range of origins, potential chemical and biological reactivity, chemical composition and solubility (Verdugo 2012). Significant proportions of sea ice DOM consist of extracellular polymeric substances (EPS), predominantly polysaccharides, the majority of which are diatom-derived (Deming 2010; Thomas et al. 2010; Aslam et al. 2012a). EPS also contribute to the POM pool (up to 72%), present as mucilage structures, cell coatings, and as self-assembling aggregates ((Krembs et al. 2002; Thomas et al. 2010; Verdugo 2012). Production of EPS is a ubiquitous characteristic of bacteria, algae, and fungi in almost all environments (water, soil, desert, benign and pathogenic biofilms), where they play numerous roles. Benefits of sea ice EPS to ice diatoms and bacteria include cryoprotection, production of salinity barriers (Krembs and Deming 2008; Aslam et al. 2012a; Ewert and Deming 2013), and creation of localised microclimates for cells (Krembs et al. 2002, 2011). EPS and dissolved carbohydrates modify the physical structure of the ice-water matrix as seawater freezes (Krembs and Deming 2008; Krembs et al. 2011). On ice melt, dissolved and particulate EPS components stimulate water-column carbon cycling (Meiners et al. 2004; Vancoppenolle et al. 2013; Niemi et al. 2014), contribute to the water column DOM pool, and through aggregation processes, influence the vertical carbon fluxes to deeper waters (Riedel et al. 2006; Assmy et al. 2013). Recent work has shown a role for EPS in the formation of atmospherically active polar aerosols (Leck et al. 2013; Wilson et al. 2015) during the open water summer period.

Understanding the contributions and key drivers in the distribution and abundance of dissolved and particulate components of the sea ice carbohydrate pool is therefore an important challenge, given the changes occurring in Arctic sea ice. To date most studies of EPS in sea ice have concentrated on the quantification of DOM, and the contribution of dissolved carbohydrate to this pool (Thomas et al. 2010; Underwood et al. 2010), or determination of transparent exopolymer particle (TEP) concentrations, which fall within the particulate EPS size fraction (Krembs et al. 2002; Meiners et al. 2004; Riedel et al. 2007). The contribution of particulate polysaccharides to total particulate organic carbon (POC) in sea ice has been reported (Krembs et al. 2002; Meiners et al. 2003, 2004; van der Merwe et al. 2009). EPS are subject to transitions between dissolved and particulate phases by physical aggregation and coagulation, hydrolysis, all influenced by environmental conditions (Chin et al. 1998; Verdugo 2012) and during processes of microbial degradation (Giroldo et al. 2003; Hofmann et al. 2009). In addition, many studies note significant spatial and temporal patchiness in biomass and concentrations of chlorophyll *a* (Chl *a*), dissolved organic carbon (DOC), POC and carbohydrates. This variability is a characteristic of many sea ice biogeochemical measurements (Rysgaard et al. 2001; Miller et al. 2015), and poses a challenge in integrating data from separate studies, and in gaining a full understanding of the overall carbohydrate budget in sea ice.

This study addressed this challenge by simultaneously measuring both particulate and dissolved sea ice carbohydrates in bottom layers of FYI across a wide area of the Canadian Arctic Archipelago, a region which represents 50% of the shelf sea region of the Arctic Ocean, with a well-described oceanographic and biogeochemical profile (Michel et al. 2006, 2015). Shelf seas are among the most productive areas of the Arctic, representing up to 85% of the total annual primary production. To be able to understand the role of EPS and carbohydrates in sea ice ecology and biogeochemistry, the first objective was to characterise the overall carbohydrate budget across a range of specific sea ice organic carbon fractions (DOC, POC, dissolved and particulate carbohydrates, including EPS and non-EPS components) for first year Arctic sea ice during the productive period of the algal spring bloom. The second objective was to determine the relationships between the carbohydrate budget and key biological characteristics and associated environmental variables (microbial community, nutrients, physical ice structure). Identifying the important drivers of different carbohydrate (including EPS and non-EPS) concentrations and composition is necessary to understand how this component of the sea-ice biome may respond under future sea ice regimes in the Arctic Ocean.

Methods
Sampling

First year sea ice was sampled in the Canadian Arctic Archipelago (Fig. 1a,b) During May 2010, 13 sites were sampled in 3 geographic locations, with 23 sites in 5 locations sampled in May 2011. Five geographic locations were sampled; Barrow Strait (BS), McDougall Sound South (MS), McDougall Sound North (MN), Resolute Passage (RP), and Wellington Channel (WC). Sites were accessed by helicopter, plane, or by snowmobile (Resolute Passage).

At each site, a number (typically between 9 and 11) of 9 cm internal diameter cores were collected with a Mark II manual corer (Kovacs Enterprises, Lebanon, New Hampshire, U.S.A.) and a suite of physical measurements taken (snow and ice thickness, upwelling and downwelling photosynthetically active radiation). For measurements of within-ice biochemical variables, the bottom 3 cm of individual ice cores at each station were removed using a stainless steel saw. Under-ice surface water was collected through core bore holes using a submersible pump held at the ice-water interface. Sea-ice samples were stored in acid-washed isothermal containers (for biomass) or sterile Whirlpak bags (nutrients, DOC, salinity), and surface-water samples were stored in acid-washed Nalgene containers.

Filtration and thawing protocols

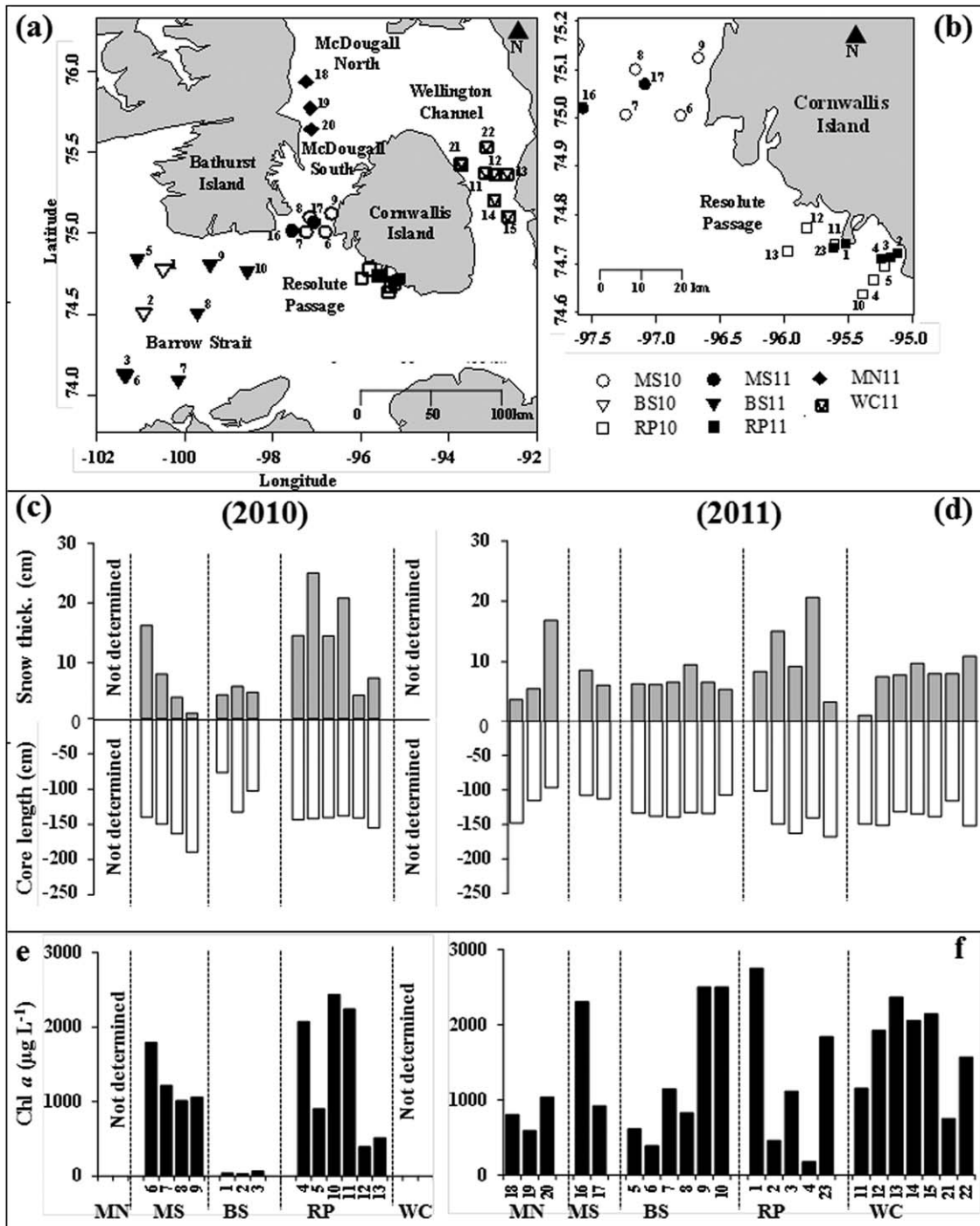For Chl *a* and POC analysis, and flow cytometric determination of microbial cell density, 3 cm thick bottom ice

Fig. 1. (**a**) Sampling stations in the Canadian Arctic Archipelago in 2010 and 2011: Barrow strait (BS), McDougall Sound South (MS), McDougall Sound North (MN), Resolute Passage (RP), and Wellington Channel (WC11, 12, 13, 14, 15, 21, 22 in 2011). (**b**) Location of sampling stations in Resolute Passage (RP). (**c**) Snow thickness (cm) and (**d**) length of individual ice cores (cm) and (**e**, **f**) Chl *a* concentrations (μg L^{-1}) in bottom sea ice for each sampling station sections collected in 2010 and 2011.

sections from a number of cores were pooled and melted slowly in darkness with addition of a known volume of 0.2 μm GF/F filtered surface sea water (FSW) collected during sampling. For analyses of DOC, nutrients, and salinity, a separate set of one or more bottom ice sections were pooled and melted in a sterile whirlpak bag at room temperature in darkness without the addition of FSW within 24 h of collection. To determine carbohydrate and EPS concentrations, a

further single ice core bottom section at each station was melted without the addition of FSW, filtered through a pre-combusted (450°C for 24 h) GF/F filter, and filtrate collected in acid-washed plastic bottles. Filters and filtrates were frozen at −20°C.

Chlorophyll *a* and organic carbon analysis

Chl *a* concentrations were determined fluorometrically (10AU Turner Designs) on duplicate subsamples filtered onto Whatman GF/F filters after 24 h extraction in 90% acetone at 4°C in the dark (Parsons et al. 1984). POC was determined on duplicate subsamples filtered on precombusted 21 mm GF/F filters and frozen at −80°C. POC samples were analysed using a Carlo Erba NC2500 Elemental Analyzer. Duplicate DOC subsamples were filtered through precombusted 25 mm Whatman GF/F filters. The filtrate was acidified with 20 μL of 50% H_2PO_4, stored at 4°C in the dark and analyzed with a Shimadzu TOC-VCHP analyzer. Total organic carbon (TOC) content was calculated by summing concentrations of dissolved (DOC) and particulate (POC) organic carbon, and the percent contribution of each dissolved and particulate organic carbon fraction were calculated with respect to TOC.

Nutrients concentrations and microbial cell densities (flow cytometry)

Filtered samples (precombusted Whatman GF/F filters) from melted ice cores were analysed for NO_3^-, NO_2^- and PO_4^{3-} (Seal's Autoanalyzer 3, Mequon, Wisconsin, U.S.A.), and $Si(OH)_4$ (Technicon II Autoanalyzer, Sydney, New South Wales, Australia) concentrations. The abundance of bacteria, nano- and picocynaobacteria and autotrophic nano- and pico-eukaryotes were determined by flow cytometry. Samples were pre-filtered through a 20 μm mesh, fixed with glutaraldehyde (0.5% final concentration, Sigma) at 4°C for 30 min, then frozen at −80°C until analysis. Bacteria samples were stained with SYBR Green I (Invitrogen) following Belzile et al. (2008) and counted with an Epics Altra flow cytometer (Beckman Coulter) fitted with a 488 nm laser operated at 18 mW. The green fluorescence of nucleic acid-bound SYBR Green I was measured at 525 +/−5 nm. Cytograms obtained were analyzed using Expo32 v1.2b software (Beckman Coulter). Pico and nano-sized autotrophic cells, including cyanobacteria, were analyzed using Epics Altra flow cytometer (Beckman Coulter) following Tremblay et al. (2009). Forward angle light scatter, right angle light scatter, orange fluorescence from phycoerythrin (575 ± 20 nm) and red fluorescence from chlorophyll (675 ± 10 nm) were measured. Pico- (< 2 μm) and nano-autotrophs (2–20 μm) were discriminated based on forward scatter calibration with polystyrene microspheres (2 μm diameter, Fluoresbrite YG, Polysciences) added to each sample as an internal standard (Tremblay et al. 2009).

Carbohydrate fraction extraction

Previously obtained filtrates were used for dissolved carbohydrates (dCHO), dissolved uronic acid (dUA) and ethanol solubility-based EPS analyses. Carbohydrates from material retained on the corresponding GF/F filters (particular carbohydrate, pCHO), were extracted using a sequence of established extraction protocols designed to separate the material into fractions on the basis of solubility and putative biological origin (Table 1).

A subsample (0.4 mL) of GF/F filtrate was used to determine total dissolved carbohydrate concentration (dCHO$_{TOTAL}$). Remaining filtrate (approximately 10–100 mL) was dialysed overnight (at 20°C) through 8 kDa dialysis tubing (VWR, U.S.A.) against ultra-pure water (18.2 MΩ, MilliQ) under moderate stirring to remove salts and smaller organic components. Dialysed material was defined as the > 8 kDa dissolved carbohydrate fraction (dCHO$_{>8kDa}$). These desalted samples were subsequently freeze-dried for EPS partitioning and determination of monosaccharide composition.

To measure the concentration of carbohydrates and uronic acids present as dissolved extracellular polymeric substances (dEPS), dialysed and freeze-dried dCHO$_{>8kDa}$ samples were re-dissolved in ultra-pure water and divided into three aliquots of 1–4 mL each. One aliquot was used to determine carbohydrate concentration and monosaccharide content (described later). The remaining two aliquots were used to isolate dEPS components with different solubility by precipitation with 30% and 70% ethanol; these precipitated EPS fractions were named as dEPS$_{complex}$, and dEPS respectively (Aslam et al. 2012a; Underwood et al. 2013). Carbohydrate not precipitated with 70% ethanol were termed dCHO$_{non-EPS}$, calculated as the difference between the concentration of dCHO$_{>8kDa}$ and concentration of dEPS for each sample.

Particulate carbohydrates (pCHO) were extracted by a sequential extraction of material collected on the GF/F filters. A hot water-extracted carbohydrate (pCHO$_{HW}$) fraction (mainly intracellular storage polysaccharides) was obtained by macerating filters in 0.5 M NaCl (salinity 30), incubation at 100°C for 1 h followed by centrifugation (3500 × *g*, 15 min). A hot bicarbonate-extracted (pCHO$_{HB}$) fraction (gelatinous and water-insoluble extracellular polysaccharides) was obtained by incubating the remaining GF/F pellet with 0.5 M NaHCO$_3$ at 100°C for 1 h followed by centrifugation (3500 × *g*, 15 min). Finally a hot alkali extraction (pCHO$_{HA}$) with 1 M NaOH and 0.2 M NaBH$_4$ at 100°C for 1 h followed by centrifugation (3500 × *g*, 15 min) dissolved the silica cell wall and liberated EPS associated with the silica frustules. Remaining material in the pellet after HA extraction was termed residual carbohydrate (pCHO$_R$) (Wustman et al. 1997; Aslam et al. 2012a). An aliquot (1 mL) of each extracted fraction (pCHO$_{HW}$, pCHO$_{HB}$, pCHO$_{HA}$, pCHO$_R$) was used to determine carbohydrate concentration (phenol sulphuric acid assay).

The remaining pCHO$_{HW}$, pCHO$_{HB}$, and pCHO$_{HA}$ extracts were dialysed overnight (at 20°C) through 8 kDa dialysis tubing (VWR, U.S.A.) against ultra-pure water (18.2 MΩ, MilliQ) under moderate stirring to remove salts and subsequently used to determine monosaccharide composition.

Table 1. Definitions and characteristics of the organic carbon and carbohydrate fractions isolated from sea ice in this study.

Fraction	Chemical characteristics	References
DOC	Dissolved organic carbon including high molecular weight extracellular polymeric substances, amino acids, other lower molecular weight compounds, e.g., acetate, and undefined compounds	Bellinger et al. (2005), Dumont et al. (2009), Verdugo (2012), Koch et al (2014)
TCHO	All dissolved and particulate carbo., including TEPs, structural polysaccharides, detritus	Dumont et al. (2009)
$dCHO_{TOTAL}$	Soluble (colloidal) fraction containing both polymeric (colloidal EPS) and non-polymeric (lower molecular weight) carbohydrates.70% monosaccharides, 30% polysaccharides	Herborg et al. (2001), Dumont et al. (2009)
$dCHO_{>8kDa}$	Hetero-polysaccharides (glucose, mannose and xylose rich) $>68\%$ EPS, 22% non-polymeric CHO	Underwood et al. (2010)
$dCHO_{<8kDa}$	Lower molecular weight material, passing through a 8 kDa filter	Present study
dEPS	Dissolved extracellular polymeric substances. Hetero-polymers (glucose, mannose, and xylose rich), gels rich in uronic acid, precipitates in 70% ethanol	Decho (2000), Underwood et al. (2010)
$dEPS_{complex}$	Hetero-polymers (glucose, galactose, mannose, and xylose rich), gels rich in uronic acid, precipitating in 30% v/v ethanol	Underwood et al. (2010, 2013)
$dCHO_{non-EPS}$	Non-precipitating extracellular polysaccharides after an EPS extraction	Underwood et al. (2013), Present study
$dUA_{>8kDa}$	48% of dCHO	Underwood et al. (2010)
$dEPS_{UA}$	Uronic acid content of dissolved EPS gels precipitating in 70% ethanol	Underwood et al. (2010)
POC	Insoluble organic carbon, high molecular weight (HMW) material including TEP	Dumont et al. (2009)
pCHO	Insoluble and HMW carbohydrate, including TEPs	Dumont et al. (2009)
$pCHO_{HW}$	Heat solubilised extracellular carbo. & intracellular glucans (chrysolaminarin), pentose/hexose rich gels	Bellinger et al. (2005), Abdullahi et al. (2006)
$pCHO_{HB}$	Gelatinous and water-insoluble extracellular polysaccharides gels; rich in deoxy sugars and uronic acids	Bellinger et al. (2005), Abdullahi et al. (2006)
$pCHO_{HA}$	Alkali extracted frustule associated polysaccharides	Present study
$pCHO_R$	Residual un-extracted carbohydrates	Present study

Carbohydrate (CHO) and uronic acid analysis

Carbohydrate concentrations in each fraction were determined using a modified phenol sulphuric acid assay (Dubois et al. 1956) as described by Aslam et al. (2012a). Glucose was used as a standard, with standard curves modified with NaCl where necessary to correspond to the salinity of the fraction being measured. Carbohydrate concentrations were calculated as glucose-carbon-equivalents and converted to μmol C L^{-1}. Uronic acids were determined by standard carbazole assay (Bitter and Muir 1962; Bellinger et al. 2005). Glucuronic acid was used as standard, and all uronic acids were expressed as glucuronic-carbon-equivalents concentrations and converted to μmol C L^{-1}.

Total carbohydrate concentrations (sum of all fractions, TCHO) were calculated by summing the carbohydrate concentration of dissolved and total particulate carbohydrate fractions, i.e., $TCHO = dCHO_{TOTAL} + pCHO$, where the total particulate carbohydrate concentration was calculated as $pCHO = pCHO_{HW} + pCHO_{HB} + pCHO_{HA} + pCHO_R$.

Monosaccharide composition of carbohydrate fractions

Neutral monosaccharide composition of desalted carbohydrate fractions was determined by gas chromatography linked with mass spectroscopy (GC-MS). Polysaccharides and standards were hydrolyzed, saponified, and then reduced to the corresponding alditols. Alditols were acetylated, and monosaccharide separation was carried out using a RT-2330 column. Inositol was used as the internal standard (Underwood et al. 2010; Aslam et al. 2012a).

Data and statistical analysis

Significant differences in variables were determined using general linear models (GLM) accounting for year of sampling and location. ANOVA with post hoc Tukey tests was used to investigate specific patterns in subsets of the data. Concentration data was log $n + 1$ transformed to minimise deviation from normality. Percentage (proportional) data were arcsin-transformed. Spearman's correlation analysis and linear regression was used to investigate relationships between different variables. A stepwise subset analysis approach was used to determine the best multiple linear regressions describing carbohydrate fraction concentrations based on potential environmental predictor (independent) variables (physical ice measurements, nutrient and Chl a concentrations, microbial cell densities). Models were compared using R^2 and predicted residual sum of squares (PRESS) values, with lowest PRESS score models selected. Because we were interested in the relative effects of potential independent

Table 2. Concentrations (μmol C L^{-1}) of organic carbon (DOC and POC), dissolved carbohydrates (dCHO$_{TOTAL}$, dCHO$_{>8kDa}$, dEPS, dUA, dEPS$_{UA}$) and particulate carbohydrate (pCHO$_{HB}$, pCHO$_{HW}$, pCHO$_{HA}$, and pCHO$_R$) in bottom sea ice sections collected from McDougall North (MC), Barrow Strait (BS), McDougall South (MS), Wellington Channel (WC), and Resolute Passage (RP) in 2010 and 2011. All values are given as mean $\pm$ SE, except MS11 where both values are given. Number of samples (n) is given underneath location name.

	Sea ice 2010			Sea ice 2011				
	MS10	**BS10**	**RP10**	**MN11**	**MS11**	**BS11**	**RP11**	**WC11**
n	4	3	6	3	2	6	5	7
Organic carbon (μmol C L^{-1})								
DOC	3008 $\pm$ 842	128 $\pm$ 30	1229 $\pm$ 141	2552 $\pm$ 862	4931–11059	4207 $\pm$ 528	2317 $\pm$ 1020	4261 $\pm$ 453
POC	5207 $\pm$ 1417	341 $\pm$ 58	3887 $\pm$ 624	2801 $\pm$ 443	3929–7192	1575 $\pm$ 399	2380 $\pm$ 375	5445 $\pm$ 857
Dissolved carbohydrates (μmol C L^{-1})								
dCHO$_{TOTAL}$	1147 $\pm$ 275	82 $\pm$ 23	627 $\pm$ 77	736 $\pm$ 115	1092–1946	1357 $\pm$ 461	504.8 $\pm$ 142.9	1290 $\pm$ 368
dCHO$_{>8kDA}$	307 $\pm$ 84	37 $\pm$ 14	236 $\pm$ 51	298 $\pm$ 84	387–524	400 $\pm$ 88	208.6 $\pm$ 69.2	446 $\pm$ 155
dEPS	42 $\pm$12	8 $\pm$ 2	57 $\pm$ 15	57 $\pm$ 5	107–169	71 $\pm$ 12	70.4 $\pm$ 24.9	109 $\pm$ 18
dUA	92 $\pm$ 16	17 $\pm$ 7	87 $\pm$ 16	175 $\pm$ 40	266–309	230 $\pm$ 61	147.6 $\pm$ 41.4	299 $\pm$ 105
dEPS$_{UA}$	15 $\pm$ 3	2 $\pm$ 1	11 $\pm$ 3	18 $\pm$ 5	33–40	31 $\pm$ 11	22.6 $\pm$ 6.6	52 $\pm$ 25
Particulate carbohydrates (μmol C L^{-1})								
pCHO$_{HB}$	50 $\pm$ 9	4 $\pm$ 0.5	16 $\pm$ 4	20 $\pm$ 7	40–59	25 $\pm$ 6	21 $\pm$ 7	30 $\pm$ 5
pCHO$_{HW}$	118 $\pm$ 17	11 $\pm$ 2.7	53 $\pm$ 10	69 $\pm$ 10	94–271	159 $\pm$ 22	79 $\pm$ 23	117 $\pm$ 13
pCHO$_{HA}$	31 $\pm$ 6	3 $\pm$ 0.5	14 $\pm$ 4	45 $\pm$ 10	65–143	63 $\pm$ 13	58 $\pm$ 10	88 $\pm$ 13
pCHO$_R$	17 $\pm$ 3	7 $\pm$ 2.4	9 $\pm$ 1	22 $\pm$ 1	23.1–23.2	27 $\pm$ 5	17 $\pm$ 4	30 $\pm$ 6

variables on sea-ice carbohydrate fractions, these analyses were conducted on standardised data (transformed into z-scores), which permits direct comparison of the magnitude of standardised multiple regression coefficients (β values) (Kocum et al. 2002). Statistical analyses were conducted in Minitab v.13.3 (Minitab). Patterns in fractional distribution of material between size components and in monosaccharide compositional data of sea ice carbohydrate fractions, and also comparisons between sea ice data and carbohydrate compositional data from axenic studies of sea ice diatoms grown in culture (data from Aslam et al. 2012a) were analysed using ANOSIM and SIMPER (Primer v.6, Plymouth, U.K.). Canonical correspondence analysis (CCA) was used to extract the major gradients present between the two multivariate sets of data available for each sampling location, namely the measurements of the relative contributions of different fractions to the overall ice carbohydrate budget, and the associated physical, chemical and biological variables (using MVSP v3.1, Kolvec Ltd, N. Wales, U.K.).

Results

Spatial and inter-annual variation in sea ice properties, algal biomass and organic carbon

All 36 sites (Fig. 1a,b) consisted of first year sea ice, ranging in thickness from 76 cm to 189 cm (Fig. 1c,d). Snow thickness was variable, between 1.1 cm and 25 cm (Fig. 1c,d). Chl *a* concentrations in the bottom 3 cm of sea ice (from the ice-water interface) ranged from 29 μg L^{-1} to 2750

μg L^{-1} (Fig. 1e,f). Bottom ice Chl *a* concentrations were significantly ($F_{1,4,40}$, $p < 0.001$) higher than those in the underlying seawater (average 0.39 $\pm$ 0.02 μg L^{-1}).

Sea-ice DOC concentrations (range 80–11,059 μmol C L^{-1}) in the bottom ice sections were significantly lower in 2010 compared with 2011 ($F_{1,4,35} = 17.3$, $p < 0.001$), with particularly low concentrations measured at Barrow Strait sites in 2010 (Table 2). Highest DOC concentrations were present in McDougal Sound South in both years (Table 2). POC concentrations were also lower in Barrow Strait in 2010, leading to a significant difference in POC concentrations between 2010 and 2011 ($F_{1,4,35} = 2.15$, $p < 0.05$), but overall, in the other regions and years (excluding Barrow Strait 2010), POC concentrations were similar (average POC = 4425 μmol C L^{-1}). Chl *a* and POC concentrations were positively correlated within the 2010 and 2011 data sets ($p < 0.001$). However, Chl *a* and DOC concentrations were not significantly correlated (Supporting Information Table S1).

Sea ice carbohydrate composition and budget

Total carbohydrate concentrations (TCHO) in sea ice varied between 55 μmol C L^{-1} and 1390 μmol C L^{-1} (mean 1114 μmol C L^{-1} $\pm$ 143 standard error). The contributions of the different dissolved and particulate carbohydrate fractions (Table 1) to the total sea ice carbohydrate budget were determined for each site (Fig. 2). Total dissolved carbohydrate concentrations (dCHO$_{TOTAL}$) exceeded particulate carbohydrate concentrations (pCHO) in all samples (Table 2), and the relative distribution of particulate and dissolved carbohydrate
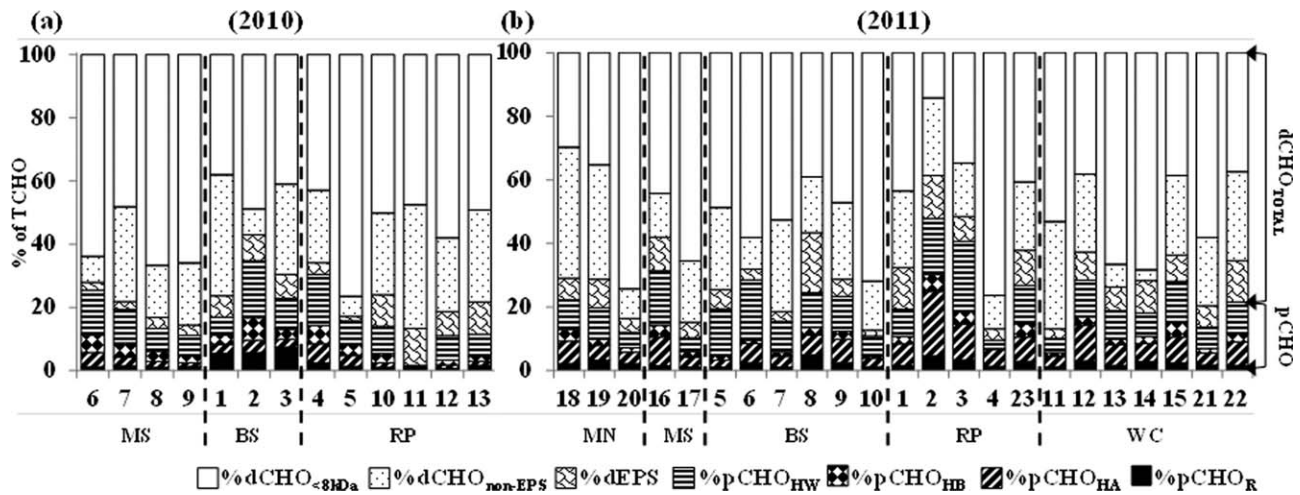
Fig. 2. Carbohydrate budget for first year arctic sea ice, showing percent contribution of dissolved and particulate fractions to the total carbohydrate profile in bottom ice sections collected from McDougall North (MN), McDougall South (MS), Barrow Strait (BS), Resolute Passage (RP), and Wellington Channel (WC) in (**a**) 2010 and (**b**) 2011. 100% $dCHO_{TOTAL}$ = %$dCHO_{<8KDa}$ + %dEPS (precipitated with 70% ethanol) + %$dCHO_{non-EPS}$. Particulate carbohydrate pCHO = $pCHO_{HW}$ + $pCHO_{HB}$ + $pCHO_{HA}$ + $pCHO_R$.

showed no significant regional or inter-annual differences (Fig. 2). Dissolved carbohydrate ($dCHO_{TOTAL}$) represented between 52% and 85% (average 77.3% ± 1.6% SE) of the total carbohydrate pool (TCHO), the largest component of which were dissolved carbohydrates < 8 kDa in size (51% ± 2.4% SE of TCHO), followed by $dCHO_{non-EPS}$ (23% ± 1.6% SE) and dEPS (7% ± 0.7% SE). $pCHO_{HW}$ was the particulate carbohydrate fraction with the greatest relative contribution to total carbohydrate content (10% ± 0.8% SE), followed by $pCHO_{HA}$ (5.5% ± 0.6% SE), $pCHO_{HB}$ (2.8% ± 0.3% SE) and $pCHO_R$ (2.3% ± 0.26% SE). There was one significant difference due to location and sampling year, in that Barrow Strait samples in 2010 had significantly higher relative abundance of $pCHO_R$ than the other locations (6.2% ± 0.63% SE, $F_{1,4,35}$ = 2.91, $p < 0.05$).

The relative consistency of the overall carbohydrate budget between sites (Fig. 2) was reflected in significant relationships between various measures of dissolved and particulate carbon. Concentrations of the six dissolved carbohydrate fractions were positively correlated with DOC (2010, 2011) and POC (in 2011) concentrations (Supporting Information Table S1). The importance of algal biomass was reflected by the presence of significant linear relationships between Chl *a* and $dCHO_{TOTAL}$ and dEPS concentrations (Fig. 3a,b, positive correlation, $p < 0.001$ in both cases) across a wide concentration range (note the logarithmic scales in Fig. 3).

Concentrations of dissolved and particulate carbohydrates in sea ice

$dCHO_{TOTAL}$ represented on average 37% of the DOC concentration pool in bottom ice. There was significant inter-annual variability; in 2010 when DOC concentrations were lower, $dCHO_{TOTAL}$ represented between 42% and

62.4% (average 52%) of the DOC pool; this proportion falling to 28.9% (range 24.7–38.1%) in 2011. Concentrations of dissolved carbohydrates > 8 kDa in size ($dCHO_{>8kDa}$) varied between 37.3 μmol C L^{-1} and 456 μmol C L^{-1}, and represented 32.5% ± 3.7% SE of the $dCHO_{TOTAL}$ content, with no significant differences between regions or years (Table 2).

Significantly higher concentrations of dUA were measured in 2011 ($F_{1,4,35}$ = 20.6, $p < 0.001$), with dUA contributing between 67% and 77% of $dCHO_{>8kDa}$ in Resolute Passage and Wellington Channel samples, whereas in McDougal Sound South in 2010, uronic acids only contributed 40% of the dissolved carbohydrate. The uronic acid components of the dEPS in ice ($dEPS_{UA}$) were a consistent 38% (SE ± 5.3%) across all sites and years. Concentrations of dissolved uronic acids (dUA) (Table 2) were closely correlated with $dCHO_{>8kDa}$ concentration (Supporting Information Table S1) in both 2010 and 2011. In bottom ice, between 8% and 75% (average 26.4%) of the $dCHO_{>8kDa}$ was present as dEPS, with $dEPS_{complex}$ representing 50% of the EPS present (data not shown).

Hot-water extracted carbohydrate concentrations ($pCHO_{HW}$) were the largest fraction of the total pCHO (mean 49.8% ± 1.7 SE), with no significant differences in the relative proportion of $pCHO_{HW}$ in pCHO between sites or years. $pCHO_{HW}$ were higher in 2011, and with significantly lower concentrations in Barrow Strait in 2010. Concentrations of $pCHO_{HB}$ did not significantly vary between years, and were consistently higher ($F_{4,1,35}$ = 4.19, $p < 0.001$) in McDougal Sound South (mean of 2010 and 2011, 50 μmol C L^{-1}) and significantly lower in Barrow Strait in 2010 (average 4.1 μmol C L^{-1}). Both $pCHO_{HA}$ and $pCHO_R$ concentrations were higher in 2011 than 2010 ($pCHO_{HA}$, $F_{4,1,35}$ = 58.0, $p < 0.001$; $pCHO_R$, $F_{4,1,35}$ = 15.3, $p < 0.001$) with $pCHO_{HA}$
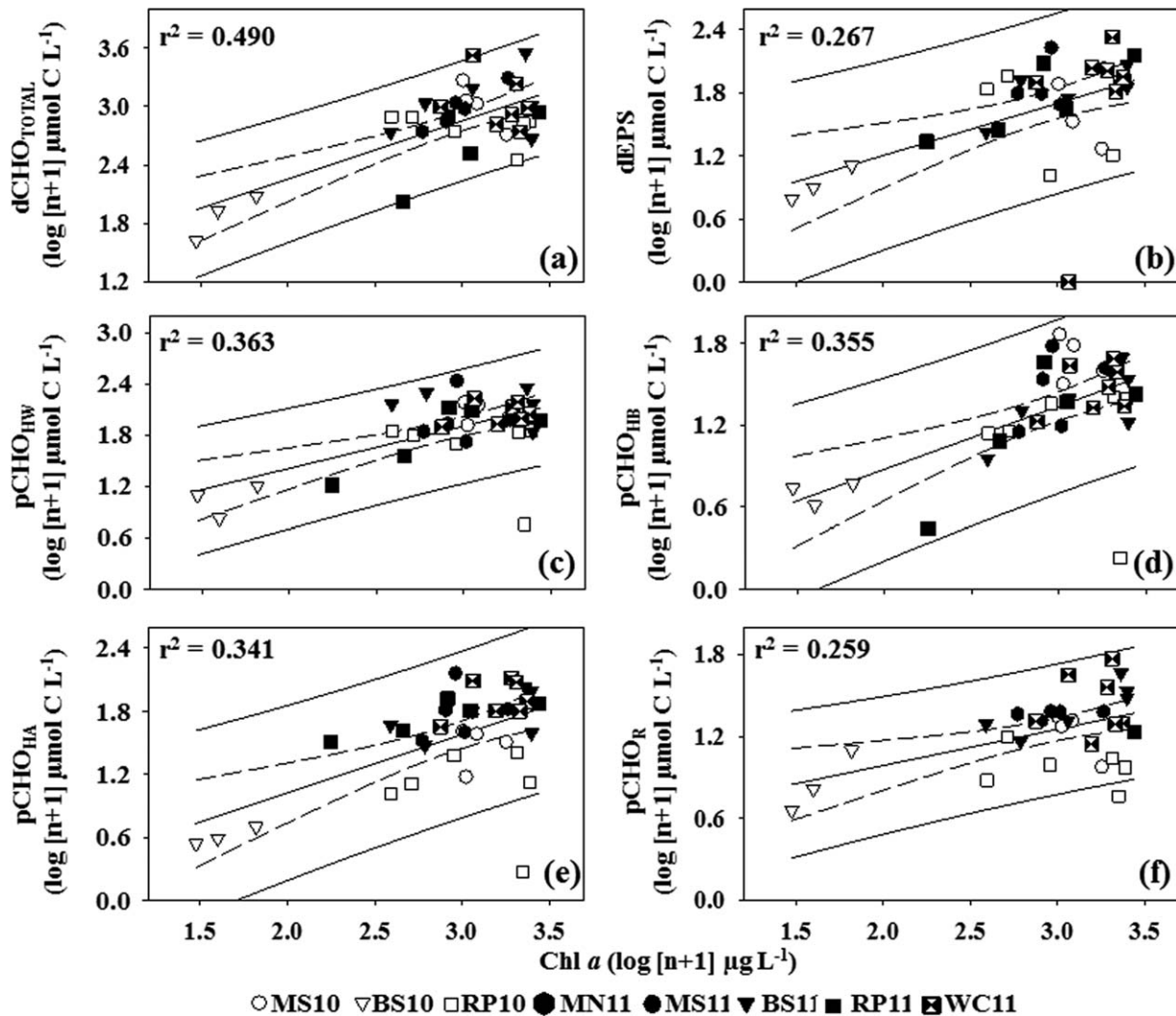
Fig. 3. Relationships between Chl a (μg L^{-1}) and carbohydrate concentrations (μmol C L^{-1}) for (**a**) total dissolved carbohydrate dCHO$_{TOTAL}$, (**b**) dEPS, EPS precipitated with 70% ethanol), (**c**) hot water (pCHO$_{HW}$); (**d**) hot bicarbonate extracted (pCHO$_{HB}$), (**e**) hot alkali (pCHO$_{HW}$) and (**f**) residual (pCHO$_R$) carbohydrate fractions. All concentration data are log transformed. Best-fit linear regression line (solid), 95% confidence limits of regression (dotted), and prediction intervals (outer lines) are shown for each relationship. Data codes as Fig. 1.

concentrations significantly lower in Barrow Strait and Resolute Passage in 2010 (Table 2).

Hot-water extracted (pCHO$_{HW}$), hot-bicarbonate-extracted (pCHO$_{HB}$) and pCHO$_R$ carbohydrates were significantly related to Chl a concentration (Fig. 3c–f, regression $p < 0.001$ except for pCHO$_R$ where $p < 0.01$). In 2011, the majority of dissolved and particulate carbohydrate fractions were positively correlated with each other (Supporting Information Table S1), although there were no significant correlations between dissolved (dCHO, dUA) and particulate (pCHO) concentrations in 2010 when DOC concentrations were lower (Supporting Information Table S1). Particulate carbohydrate concentrations consistently represented an average of 6.5% ± 0.6% SE of the POC concentration, except in Resolute Passage in 2011, where pCHO was 11.3% of the POC.

Carbohydrate concentrations (both particulate and dissolved) in melted bottom sea ice sections were one to two orders of magnitude higher than concentrations in underlying sea water. Seawater carbohydrate concentrations were low (average concentrations of dCHO$_{>8kDa}$, dUA and pCHO were 17.4 ± 0.81, 6.52 ± 0.51, and 3.1 ± 0.21 μmol C L^{-1} ± SE, respectively), with no significant differences in concentrations between regions or years (data not shown).

Monosaccharide composition of carbohydrate fractions

As well as the differences in concentrations and relative contributions to the overall carbohydrate budget, the various carbohydrate fractions had significant differences in their constituent monosaccharides (ANOSIM global R, 0.695, $p < 0.001$). Glucose, mannose, and xylose were the most

abundant monosaccharides present in the dCHO$_{>8kDa}$, pCHO$_{HW}$, pCHO$_{HB}$ and pCHO$_{HA}$, together contributing over 75% of the total monosaccharide pool (Fig. 4). These four carbohydrate fractions had significantly different monosaccharide profiles; dCHO$_{>8kDa}$ were primarily separated from pCHO$_{HW}$ and pCHO$_{HB}$ fractions by being glucose rich, followed by differences in galactose and mannose content (Fig. 4a); pCHO$_{HA}$ extracts being mannose and xylose-rich (Fig. 4d), pCHO$_{HB}$ fractions being more xylose, fucose, arabinose and galactose-rich (Fig. 4c), and pCHO$_{HW}$ extracts (Fig. 4b) occupying an intermediate position with more rhamnose and ribose (R statistic, dCHO$_{>8kDa}$ vs. pCHO$_{HB}$, 0.966; vs. pCHO$_{HA}$, 0.958; vs. pCHO$_{HW}$, 0.895, $p < 0.001$).

There were no significant differences (ANOSIM and SIMPER) between the monosaccharide composition of sea ice carbohydrate fractions and carbohydrate and EPS fractions produced by log and stationary phase axenic cultures of three sea ice diatoms, *Fragilariopsis cylindrus*, *F. curta*, and *Synedropsis* sp. (Table 3, culture data from Aslam et al. 2012a). Ice dCHO$_{>8kDa}$ was similar in composition to hot-water extracted carbohydrate produced by *F. cylindrus* and *Synedropsis* sp. and the extracellular dissolved carbohydrate (equivalent to dCHO$_{>8kDa}$) produced by *Synedropsis* sp. (Table 3). Ice pCHO$_{HB}$ composition was similar to extracellular dissolved carbohydrate and hot-bicarbonate extracted carbohydrates from *F. cylindrus*, *F. curta* and *Synedropsis* sp., and the hot alkali-extracted carbohydrates from *Synedropsis* (Table 3). Ice pCHO$_{HA}$ was very similar (80.5%) to the composition of carbohydrates extracted using hot alkali from the frustules of *F. cylindrus*. Of the four field-measured carbohydrate fractions, only the sea ice pCHO$_{HW}$ fraction was significantly different in composition to the ice diatom culture extracts.

In contrast to sea ice material, carbohydrate present in underlying seawater was mainly comprised of mannose, glucose and xylose (Supporting Information Fig. S1a–d). All the sea water fractions were significantly different in composition from the corresponding bottom ice extracts (ANOSIM, Global $R = 0.441$, $p < 0.001$). The greatest differences were between the dCHO$_{>8kDa}$, pCHO$_{HW}$ and pCHO$_{HB}$ fractions in ice and seawater (mean $R = 0.585$, $p < 0.001$), with the pCHO$_{HA}$ fractions from seawater and bottom ice least different (mean $R = 0.239$, $p < 0.001$).

Variability in concentrations by site, region and between-years

Patchiness was a key feature in the distribution of ice algal biomass; differences between individual sites representing 68.8% of the variation in concentration, compared with variability between regions and years (19.5% and 11.7% of the variability respectively). The average coefficient of variation (c.v.) in Chl *a* concentrations was 0.64, but ranged from 0.27 in McDougal Sound South 2011 to 0.94 in Resolute Passage in 2011. Chl *a* concentrations in ice from Barrow Strait in 2010 were significantly lower than all other regions and
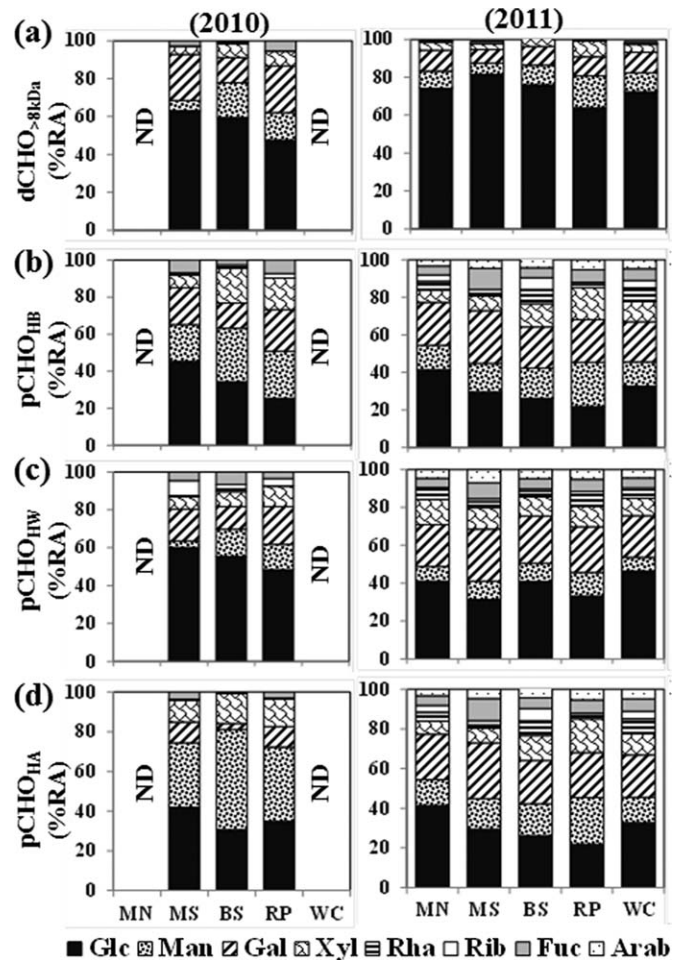

Fig. 4. Relative abundance (%) of neutral monosaccharides in (**a**) dissolved carbohydrate (dCHO$_{>8kDa}$), (**b**) hot bicarbonate (pCHO$_{HB}$), (**c**) hot water (pCHO$_{HW}$) and (**d**) hot alkali (pCHO$_{HA}$) extracted fractions in bottom sea ice and underlying seawater samples collected from McDougall North (MN), McDougall South (MS), Barrow Strait (BS), Resolute Passage (RP), and Wellington Channel (WC) in 2010 and 2011.

years ($F_{1,4,35} = 5.11$, $p < 0.05$), but otherwise, there were no significant differences between regions, with an average sea ice Chl *a* concentration of 1269 μg L^{-1}.

Similar levels of variability were measured in total dissolved carbohydrate concentrations, with 68.4% of the variation due to inter-site variation, with regions and years accounting for 18.8% and 12.8% of the variability respectively. The c.v. of dCHO$_{TOTAL}$ was high, 0.82. Very similar partitioning of variance was present for the individual fractions of dissolved carbohydrates (data not shown), due to the high levels of correlation between dissolved fractions and dCHO$_{TOTAL}$ (Supporting Information Table S1). There was a strong inter-annual difference in total particulate CHO concentrations (explaining 32% of the total variance), with significantly lower concentrations of all four pCHO fractions in 2010 (see previous sections). Particulate carbohydrates

Table 3. Percent similarity (ANOSIM and SIMPER) between monosaccharide profiles of dissolved (dCHO$_{>8kDa}$) and particulate carbohydrate fractions (pCHO$_{HW}$, pCHO$_{HB}$, pCHO$_{HA}$) extracted from Arctic sea ice, and the monosaccharide profiles of four different carbohydrate extracts (colloidal carbohydrate (CC) equiv. to dCHO$_{>8kDa}$, hot water (HW), hot bicarbonate (HB) and hot alkali (HA)) from axenic log and stationary phase cultures of three polar sea ice diatoms taxa, *Fragilariopsis cylindrus*, *F. curta* and *Synedropsis* sp. (data from Aslam et al. 2012a). $n = 144$ samples of field data, $n = 64$ for culture data. Pairwise comparisons not significantly different are indicated (i.e., they are similar). - = significant dissimilarity, pairwise comparisons between field and culture data were different ($p < 0.05$ or greater).

Sea ice carbohydrate fraction	Sea ice diatom taxa		
	F. cylindrus	*F. curta*	*Synedropsis* sp.
dCHO$_{>8KDa}$	HW, 72.3%	-	CC, 74.3%
			HW, 77.9%
pCHO$_{HW}$	-	-	-
pCHO$_{HB}$	CC, 74.2%	CC, 70.1%	HB, 75.4%
	HB, 68.8%	HB, 73.7%	HA, 75.8%
pCHO$_{HA}$	HA, 80.5%	-	-

also showed a stronger level of variation partitioning due to location (20% of variance, $p < 0.05$), caused not only by low biomass in Barrow Strait in 2010, but also differences in concentration between McDougall Sound South and Resolute Passage (see previous sections). The overall coefficient of variation for total pCHO concentration was 0.60.

Relationship between sea ice carbohydrate concentrations and physical, chemical and biological variables

The abundance of nanoeukaryotes and PO$_4^{3-}$ concentration (Supporting Information Table S2) were equally important significant positive variables describing the (standardised) concentrations of total dissolved carbohydrate (Table 4). Nanoeukaryote abundance was the most significant predictor of the concentration of dCHO$_{>8kDa}$ and of dissolved uronic acids (Table 4). The best fit model to predict dEPS concentration (R^2 of 39.6%) was driven positively by total protist abundance ($\beta = 0.48$) and NO$_3^-$ ($\beta = 0.36$) concentration, and negatively by ice core salinity ($\beta = -0.29$).

Total bacterial abundance was the strongest significant positive factor in predicting the concentrations of particulate carbohydrates (pCHO, pCHO$_{HW}$, pCHO$_{HB}$) in sea ice (Table 4). Nanoeukaryote density was also a positive variable in models for pCHO, pCHO$_{HW}$ (Table 4), with similar relative importance to total bacteria. Increasing pCHO$_{HB}$ concentrations were strongly positively influenced by increasing concentrations of silicate, with nitrate concentration having a weaker negative relationship. Nanoeukaryote abundance and

to a lesser extent, nitrate concentration, were positive factors in influencing pCHO$_{HA}$ concentrations. Increases in the relative amount of pCHO$_{HA}$ (%pCHO$_{HA}$) were associated with increased snow thickness, total protist abundances, and increased nitrate concentrations, and negatively with Chl *a* concentration (Table 4).

There were significant patterns between the relative contribution of each carbohydrate fraction to the total carbohydrate pool (the carbohydrate budget, Fig. 2) and environmental variables across all 36 sites (Fig. 5, CCA explaining 66.2% of the cumulative constrained eigenvalues, with significant correlations ($p < 0.001$) between fraction contribution and environmental variables on CCA1 and CCA2). The first canonical correspondence axis (CCA1) represented a significant gradient of increasing importance of dissolved carbohydrate fractions, correlated with measures of microbial biomass (abundances of nano- and pico- cyanobacteria and eukaryotic autotrophs), and with silicate and phosphate concentrations (Fig. 5). The centroids representing particulate carbohydrate fractions (pCHO$_{HW}$, pCHO$_{HB}$, pCHO$_{HA}$, and pCHO$_R$) were located toward the negative end of the CCA1 gradient, and were associated with higher nitrate concentrations and higher salinity and thicker ice. Canonical Correspondence Axis 2 was positively correlated with increasing phosphate, silicate, ice thickness, and total Bacteria, nano-cyanobacteria and nano-eukaryotes. Relative abundance of the larger size fractions of dissolved carbohydrates (dCHO$_{>8kDa}$ and dEPS) were negatively associated with the CCA2 gradient (Fig. 5). Chl *a* data were included in the CCA (all environmental data available was used) but it was not significantly correlated with CCA1 or CCA2, because this analysis was concerned with the relative contribution of carbohydrate components to the overall budget, not the concentration of the carbohydrate fractions, which were correlated with Chl *a* (Fig. 3).

Individual site samples were positioned across these CCA gradients, with no clear groupings by location (as supported by the previous analyses), but with differences in the carbohydrate budget of individual samples dependant on the strong environmental and biochemical drivers represented in the CCA. Many samples from MS10 and MS11, RP10 and BS11 tend toward the biomass-rich, dissolved carbohydrate-dominated areas of the plot (positive CCA1 and CCA2), whereas many of the individual BS10, WC11 and RP11 samples were located in regions with a relatively greater importance of more complex particulate carbohydrate fractions associated with lower microbial densities, thicker ice and higher nitrate concentration regions of the plot. Despite Barrow Strait 2010 (BS10) being characterised by significantly lower concentrations of many of the biochemical variables measured (Table 2; Fig. 3; Supporting Information Table S1, previous sections), BS10 samples were not "outliers" in terms of the relationships between relative contributions of different carbohydrate fractions to the carbohydrate budget and

Table 4. Standardised multiple regression analysis, showing statistically significant regressions (all $p < 0.05$ or less) between dissolved and particulate sea ice carbohydrate fractions (carbo. fraction) and environmental variables in the combined 2010–2011 data set. Significance of the standardised multiple regression coefficient (β) for each variable in the regression, $p < 0.05^*$, $< 0.01^{**}$ and $< 0.001^{***}$.

Carbo. fraction	Variable	β	p	R^2	Carbo. fraction	Variable	β	p	R^2
$dCHO_{TOTAL}$	Nanoeukaryotes	0.57	***	69.2	pCHO	Total bacteria	0.46	*	58.9
	$[PO_4^{3-}]$	0.62	***			Nanoeukaryotes	0.39	*	
	Chl a	−0.33	*		$pCHO_{HW}$	Total bacteria	0.43	0.053	42.8
$dCHO_{>8kDa}$	Nanoeukaryotes	0.78	***	59.2		Nanoeukaryotes	0.31	0.12	
dUA	Nanoeukaryotes	0.75	***	53.2	$pCHO_{HB}$	$[Si(OH)_4]$	0.52	***	77.1
dEPS	Total protists	0.48	**	39.6		Total bacteria	0.54	***	
	$[NO_3^-]$	0.36	*			$[NO_3^-]$	−0.20	*	
	Core salinity	−0.29	0.08		$pCHO_{HA}$	Nanoeukaryotes	0.64	***	50.7
						$[NO_3^-]$	0.25	***	
					$\%pCHO_{HA}$	Snow thickness	1.1	***	58.4
						Total protists	0.9	***	
						$[NO_3^-]$	0.55	**	
						Chl a	−0.73	**	

environmental variables (Fig. 5), but represent a genuine part of the continuum from low to high biomass sea ice samples investigated in this study.

Discussion

The rapid rate of environmental change in high latitude northern polar regions (Polyakov et al. 2012) will increase the area of first year sea ice and seasonal ice zones across the Arctic basin, changing the annual ecology and biogeochemistry of this region (Clark et al. 2013). The important role played by carbohydrate-rich constituents (and particularly different EPS fractions) in sea ice ecology and biogeochemistry has been increasingly recognised in the last few years (Krembs et al. 2011; Underwood et al. 2013; Vancoppenolle et al. 2013). There is also growing evidence that sea ice EPS can influence the fate of carbon in post ice melt water column biology (Riedel et al. 2006; Assmy et al. 2013; Niemi et al. 2014) and is linked to aerosol formation and ocean-atmosphere interactions (Russell et al. 2010; Leck et al. 2013; Wilson et al. 2015). This study, the first simultaneous investigation of the concentrations, composition and inter-relationships between dissolved and particulate carbohydrates fractions, microbial composition and physical and chemical variables enables the production of an overall carbohydrate budget for Spring first year Arctic sea ice, and an understanding of the drivers of these relationships (Fig. 6).

Composition of carbohydrates and EPS in sea ice

Seawater DOM exhibits a continuum of size and solubility, determined in part by chemical composition of the molecules concerned, aggregation and dis-aggregation between dissolved and particulate forms influenced by factors such as salinity and ionic composition (Decho 2000; Verdugo 2012).

The size fractionation process we used was developed from studies of diatom EPS production (Wustman et al. 1997; Abdullahi et al. 2006; Aslam et al. 2012a), and successfully applied to sea ice samples (Underwood et al. 2010; Aslam et al. 2012b). This process separates DOM into fractions (Table 1) that correspond to major categories of DOM and EPS derived from micro-organisms (Underwood and Paterson 2003; Aslam et al. 2012a,b; Ewert and Deming 2013). The majority (mean 77%) of the carbohydrates present in the bottom layers of sea ice were in dissolved form ($dCHO_{TOTAL}$), the remainder being present in various particulate fractions (Fig. 6). A large proportion (about 68%) of the $dCHO_{TOTAL}$ present in sea ice passed through 8 kDa dialysis membrane (8 kDa represents a polysaccharide of approximately 40 monosaccharide units in length), which is a small molecular size compared with the polysaccharides (containing thousands to tens of thousands of monosaccharides) implicated in formation of gels and structures (McConville 1985; Hoagland et al. 1993; Verdugo 2012). High concentrations of these dissolved lower-molecular weight carbohydrates are indicative of actively photosynthesising algal assemblages, for example in biomass-rich meltwater ponds in Antarctic sea ice (Underwood et al. 2010), and in productive intertidal autotrophic biofilms (Perkins et al. 2001). The freshly produced lower molecular weight exudates in diatom-dominated assemblages are highly labile, supporting the microbial (i.e., bacterial) food web (Haynes et al. 2007; Hofmann et al. 2009; Niemi et al. 2014), although they differ from the EPS components that contribute to altered ice properties (Krembs and Deming 2008; Krembs et al. 2011). Carbohydrate-rich dEPS represented around 26% (range 8–75%) of the carbohydrate in the $dCHO_{>8kDa}$ fraction, lower than in Antarctic sea ice (68%, Underwood et al. 2010). Although the concentrations
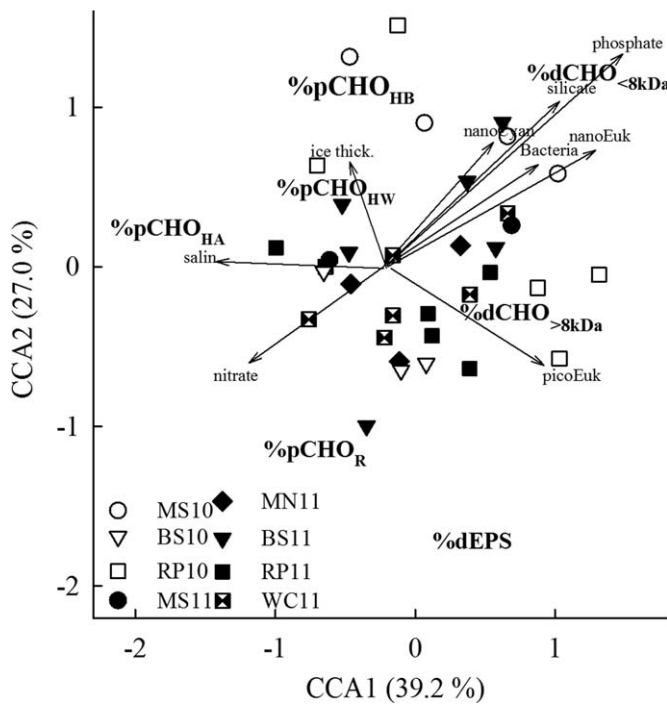
Fig. 5. Canonical correspondence analysis triplot of the percentage contribution of different carbohydrate fractions (bold font) to total carbohydrate content in first year sea ice and quantitative environmental variables (vectors), based on 36 samples taken from five locations during May 2010 and 2011 (symbols). Carbohydrate fraction – environmental correlations of 0.68 and 0.73 for CCA1 and CCA2, respectively (both $p < 0.001$).

Fig. 6. Summary carbohydrate budget and biological and environmental drivers in the bottom layers of first year sea ice during Spring, showing the distribution of carbon between a range of dissolved and particulate size fractions (middle column). Left-hand column shows environmental drivers of carbohydrate concentrations (+ and − ve) and the correlations with Chl *a* concentration (*** = $p < 0.001$; ** = $p < 0.01$). Right-hand column shows positive drivers that influence the relative contribution (% rel. cont.) of sea-ice carbohydrates fractions to the overall ice carbohydrate budget.

of dEPS in the Canadian Archipelago are relatively high compared with other polar sea ice regions that have been studied (Underwood et al. 2013), the lower proportions of dEPS relative to the total in these Arctic sea ice samples, are a result of the higher levels of production of more labile dissolved carbohydrate components by the actively growing bottom ice algae assemblages in light and nutrient conditions suitable for growth (Smith et al. 1993; Michel et al. 1996).

The dEPS in the bottom ice layers was predominantly complex EPS (dEPS$_{complex}$) and had both a relatively high uronic acid content, and a glucose-rich monosaccharide composition. Uronic acids provide a structural element in EPS, due to facilitating cross linking of polysaccharide chains via cation bridges (Sutherland 2001), which contributes to some of the cell-protective properties of microbial EPS (Steele et al. 2014). The general patterns for the first year Arctic ice sampled here, with strong correlations between uronic acid, dCHO and dEPS concentrations, and uronic acids accounting for 38% of the dCHO, matches similar data from Antarctic sea ice (uronic acid contribution to dCHO of 37–48%, Underwood et al. 2010, 2013). Benthic diatoms produce lower proportions of uronic acids within their dEPS ($< 5\%$ contribution, Abdullahi et al. 2006), with higher proportions (10–25%) in their pCHO fractions (Abdullahi et al. 2006;

Poulsen et al. 2014), but also increase the uronic acid content when salinity and nutrient stressed (Abdullahi et al. 2006). Higher uronic acid content in sea ice dCHO suggests that sea ice diatoms may incorporate more uronic acids in their EPS than benthic diatoms (salinity in brine channels can exceed 50), but could additionally indicate a contribution from uronic-acid rich bacterial EPS in this fraction (see later in discussion).

Many authors have measured transparent exopolymer particles (TEP) in sea ice (Krembs et al. 2002; Meiners et al. 2004; Riedel et al. 2007). In our study, a proportion of polysaccharide aggregates falling within the description of TEP would be retained on the GF/F filters used to separate dissolved and particulate forms (Verdugo 2012), in addition to the cellular material present in the sea ice microbial assemblages. TEP contains a mixture of material from a range of sources, and can be formed by a range of reversible aggregation reactions within the water column (Verdugo 2012). It is possible some TEP present in the melted ice cores could have disaggregated and passed through the filters we used.

Quantitative staining of TEP is undertaken using xanthan gum standards, which can be calibrated against glucose in the phenol-sulphuric acid assay (Krembs et al. 2011). Depending of their solubility, any TEP on the filters are likely to be extracted primarily in the pCHO$_{HW}$ and pCHO$_{HB}$ fractions, which extracts polysaccharides of increasing insolubility (Wustman et al. 1997; Chiovitti et al. 2005; Abdullahi et al. 2006). It is not therefore possible to separate the contribution of TEP from the diatom-cell associated carbohydrates in these fractions. pCHO$_{HW}$ and pCHO$_{HB}$ together constituted about 15% of the total carbohydrate budget (Figs. 2, 6), but made up the majority of the pCHO (60–70%). pCHO$_{HW}$ extracts from diatom cultures are predominantly glucose (Chiovitti et al. 2004; Underwood et al. 2004; Abdullahi et al. 2006), but field extractions of pCHO$_{HW}$ include other monosaccharides (e.g., galactose, xylose), that may be extracellular material (including solubilised TEP), co-extracted with intracellular storage compounds (Bellinger et al. 2009; Underwood et al. 2010). This mix of material from various sources in the pCHO$_{HW}$ extracts explains why this particular fraction did not show any close similarity to carbohydrate fractions extracted from axenic cultures of sea ice diatoms (Table 3).

The pCHO$_{HB}$ extraction method solubilises complex EPS structures (pads, coatings etc.) (Wustman et al. 1997; Bellinger et al. 2005), including more recalcitrant TEP, and had a monosaccharide composition including mannose, rhamnose, fucose, xylose, arabinose, consistent with the structural role of these EPS (Zhou et al. 1998; Aslam et al. 2012a; Liu et al. 2013). The solubility characteristics, monosaccharide and uronic acid composition of the main dEPS and pCHO$_{HB}$ components isolated from the first year arctic sea ice matches those properties of mucilage EPS shown to affect ice crystal and brine channel formation (Krembs and Deming 2008; Krembs et al. 2011), and in forming sticky brine channel plugs (Krembs et al. 2002; Juhl et al. 2011) and protective envelopes for microbial cells (Aslam et al. 2012a; Liu et al. 2013; Steele et al. 2014). The pCHO$_{HA}$ extraction dissolves the silica frustules of diatoms and liberates the polysaccharides intimately associated with the frustule (Chiovitti et al. 2005). Culture studies have found pCHO$_{HA}$ to be highly enriched with mannose (often glucurono-mannan composites) (Wustman et al. 1997; Chiovitti et al. 2005; Aslam et al. 2012a), and the sea ice pCHO$_{HA}$ extracts were also mannose rich. Concentrations of ice pCHO$_{HA}$ were strongly related to the abundance of nano-eukaryotes, a size category predominantly consisting of diatoms (Poulin et al. 2011). pCHO$_{HA}$ would be susceptible to microbial degradation after frustule dissolution and contribute part of the carbon transfer to the benthos in settling organic matter after ice melt (Juul-Pedersen et al. 2008).

Overall, the pCHO$_{HW}$ and pCHO$_{HB}$ fractions constituted approximately 60–70% of the pCHO, but only 6.5% of the POC. Other studies have found a much greater proportional contribution of pEPS (i.e., TEP) to POC than we report here (Meiners et al. 2003; Riedel et al. 2006; van der Merwe et al. 2009). As the concentrations of pCHO$_{HW}$ and pCHO$_{HB}$ measured in the current study are high, it would appear that the higher POC in the sea ice must consist of non-carbohydrate organic carbon, such as microbial cell walls (e.g., peptidoglycan cell walls, chitin element in diatoms) that would not be detected by the phenol-sulphuric acid assay, plus refractory detrital material, potentially incorporated during ice formation. Sea ice forming close to land over shelf areas of the Arctic contains sediments mixed by storms into the water column (Kempema et al. 1989), which may partly explain the higher contribution of pEPS to POC in published Antarctic and Fram Strait studies compared with the values determined in this study.

Inter-relationships between carbohydrates, microbial assemblages, physical and environmental variables in sea ice

We sampled first-year ice, either pack ice or landfast ice, at distributed stations in channels of the Canadian Archipelago. Algal biomass was high in Resolute Passage, and typical for this area of high mixing and nutrient input (e.g., Cota et al. 1987; Smith et al. 1993; Piwosz et al. 2013). The Barrow Strait 2010 values are not atypical for offshore pack ice (Meiners et al. 2003; van der Merwe 2009; Underwood et al. 2010), with high spatial and inter-annual variability a common feature of Arctic sea ice.

Despite high spatial variability, the concentrations of all carbohydrate fractions were closely correlated to DOC concentrations (indicating that the proportion of carbohydrate within the DOC pool is relatively consistent), and pCHO to POC and Chl *a* concentrations. Overall dCHO$_{TOTAL}$ represented 37% of the DOC, similar to values determined in the Antarctic (31%, Herborg et al. 2001; 39–41% Underwood et al. 2010). While Chl *a* is a key variable in determining carbohydrate content in sea ice (as algae are major carbohydrate and EPS producers, Ewert and Deming 2013; Underwood et al. 2013; Vancoppenolle et al. 2013), there was not a significant correlation between Chl *a* and DOC concentration. At large sampling scales, major biomass indicators are correlated (Underwood et al. 2013), but a degree of uncoupling in Chl *a*, DOC and carbohydrate concentrations has been previously observed (Krembs et al. 2002; van der Merwe et al. 2009; Underwood et al. 2010), relating to the high levels of spatial and temporal patchiness of individual ice core measurements (Rysgaard et al. 2001; Vancoppenolle et al. 2013). DOC contains a wide variety of compounds, not exclusively derived from algal activity, such that the DOC content in any particular ice section may be a product of the past history of that section of ice (for example, the residue of an active algal bloom that has senesced) or derived from an alternative source of organic carbon. Algal biomass is driven by a number of key factors, primarily light and nutrient

availability. Local drivers such as salinity, snow cover and ice thickness are key factors regulating ice algal patchiness at different scales (Gosselin et al. 1986; Granskog et al. 2005; Campbell et al. 2014). Ice thickness has been found to be a good general predictor of ice Chl *a* and dissolved carbohydrate content at large geographical scales (Meiners et al. 2012; Underwood et al. 2013), and was a driver for increased relative contribution of $pCHO_{HW}$ and $pCHO_{HB}$ in this study (Fig. 6). We found that increased snow cover increased the $\%pCHO_{HA}$, presumably due to a reduction in the activity of autotrophs and thus reduced production of dissolved extracellular carbohydrate components.

Although there was a clear relationship between Chl *a* and carbohydrate concentrations (Fig. 3), stepwise standardised multiple regression found that cell abundances and certain nutrient concentrations were better predictors of concentration than Chl *a* for certain sea ice carbohydrate fractions (Table 4). Chl *a* is often used as a proxy for biomass, but Chl *a* cell^{-1} varies with light and cell physiological status (Geider et al. 1998), which would therefore be affected by both the historical development of sea ice each year and current and recent conditions at each location when sampled. This indicates that the abundance of particular groups of microorganisms (in our study nanoeukaryote abundance was particularly important) and their physiological state will significantly influence the nature of the carbohydrate pool within an area of sea ice. This conclusion does not contradict statements that sea ice carbohydrate concentrations are closely related to Chl *a* concentrations (as shown in Fig. 3), only that finer scale resolution of the autotrophic assemblage composition derived from flow cytometry provides better predictive power, as determined by stepwise regression. The autotrophic protist species composition in these bottom ice layers is well described, with pennate diatoms representing the major constituents of the assemblages (Riedel et al. 2003; Niemi et al. 2011; Poulin et al. 2011). There is a broad diversity of picoeukaroytes and nano- and picocyanobacteria present in Archipelago sea ice (Piwosz et al. 2013), but nanoeukaryotes, mainly pennate diatoms, were dominant in the samples in our study (visual observation in each core, M. Poulin and C. Michel, unpubl.) and identified as major drivers in five out of six significant regressions for dissolved carbohydrate fractions (Table 4). Important diatom taxa at these locations are *Nitzschia frigida*, *Entomoneis kjellmannii*, *Fragilariopsis cylindrus*, *Cylindrotheca closterium*, *Navicula directa*, with occasional occurrences of the colonial centric *Melosira arctica* (Poulin et al. 2011, 2014). The importance of diatoms in the nanoeukaryote assemblage is supported by the close similarity in the monosaccharide composition of the sea ice carbohydrates (especially $dCHO_{>8kDa}$ and $pCHO_{HB}$) with those from axenic culture studies of sea ice diatoms (Aslam et al. 2012a), and in the relative amounts of $dEPS_{complex}$, and dEPS present. The culture data includes a range of characterised carbohy-

drate fractions produced in both log and stationary phase by the three diatom species (Aslam et al. 2012a). The close agreement between field and culture measurements (Table 3), and the major differences between sea ice carbohydrate profiles and those from seawater underlying the ice, provides additional indirect evidence that in actively growing ice communities, production of EPS and other dissolved compounds is primarily driven by diatoms in bottom ice microbial assemblages.

Bacterial abundance was a driver in three out of six significant regressions for particulate carbohydrate fractions. Bacteria play an important role in ice community dynamics, producing a range of uronic acid-rich dEPS, degrade algal EPS and DOC (Ewert and Deming 2013; Niemi et al. 2014), including selective degradation of particular monosaccharide components (Giroldo et al. 2003), and can also stimulate EPS production by diatoms (Bruckner et al. 2011). Bacteria density was associated with the measures of autotrophic and nanoplankton (cyanobacterial and eukaryotic) density. The presence of an active microbial-loop in sea ice brine channels (Ewert and Deming 2013) indicates the close interdependence of all these variables. Sea ice bacterial-EPS is uronic acid-rich and provides structural and protective functions to the bacterial cells (Mancuso Nichols et al. 2005; Aslam et al. 2012b; Ewert and Deming 2013). Many of these EPS will be extracted in the $pCHO_{HW}$ and $pCHO_{HB}$ fractions, where high numbers of bacteria will generate a proportion of the total yield of these fractions. Close correlations have been reported between bacterial density and TEP (Meiners et al. 2004), DOC and EPS (Krembs et al. 2002), but not in old multiyear ice (Meiners et al. 2003). Bacteria and picoplankton components appear to be more important in different seasons of the year (Piwosz et al. 2013), particular during winter months when heterotrophic activity is relatively greater (Niemi et al. 2011; Paterson and Laybourn-Parry 2012), whereas the current study was conducted during the period of maximum autotrophic biomass and production (Lavoie et al. 2005).

Consequences of future changes in sea ice conditions on carbohydrate budgets

We have found clear underlying patterns in the distribution and composition of sea ice carbohydrate that are broadly consistent and are influenced by a number of key drivers including the composition of the autotrophic microbial ice assemblage, nutrient concentrations, and ice thickness (Fig. 6). Changes in sea ice cover in the Arctic Ocean caused by accelerated regional warming offer two scenarios to consider. First, the loss of multiyear ice (Polyakov et al. 2012), and refreezing of areas of open water formed during summer, will result in greater areas of first year ice (Stroeve et al. 2014; Swart et al. 2015). Such ice can support more productive ice algal communities than multiyear ice, particularly in younger ice formed in refrozen leads (Lange et al.

2015). Comparison of the diversity of diatom assemblages found no significant differences between winter first year and multi-year ice (Werner et al. 2007), with pennate diatoms dominant in both types of ice, suggesting that the algal composition of these new areas of first year ice would not be dissimilar to those found in present areas of annual ice. Concurrent reduction in snow cover (Hezel et al. 2012) would further enhance ice algae growth within existing and new areas of first year ice. Increased ice algae production will result in increased abundance of carbohydrates, particularly lower molecular weight labile components to support microbial (i.e., bacterial) activity, and larger refractory EPS with enhanced cell-protection qualities. The consistent drivers identified in this study for first year spring ice carbohydrate budgets, implies that a shift from multi-year to first-year ice may result in increasing microbial primary and secondary production in high latitude Arctic areas.

Second, Arctic warming is associated with an overall thinning of the sea ice, potentially with later freezing and earlier melt. Our study found that thicker ice supports less algal biomass, proportionally less $dCHO_{<8kDa}$ material and more complex EPS and particulate EPS constituents. Therefore future scenarios of overall thinner Arctic sea ice will enhance the diatom-driven characteristics of first year carbohydrate budgets, enhancing biochemical processes within the sea ice and on release to surface waters.

Concentration and composition of sea ice carbohydrate is important not only during the period of ice cover, but also when sea ice melts and provides the open water column with organic compounds, nutrients and cells (Michel et al. 2006; Vancoppenolle et al. 2013). Earlier melt of Arctic sea ice (Stroeve et al. 2012; Stroeve et al. 2014) would coincide with an earlier flux of sea-ice constituents to the water column. The composition of the carbohydrate present as DOC in the seawater underneath the ice was very different from the material present in the bottom ice layers. The low concentrations of seawater DOC and CHO_{TOTAL} in this study, which contained little lower molecular weight material, and with profiles similar to $pCHO_{HA}$, suggest some minimal input of detrital cell material from the ice layer plus typical ocean water levels of refractory DOC (60 μmol L^{-1}). The labile carbohydrate flux during ice melt could stimulate the growth of surface water bacteria (Amon et al. 2001; Niemi et al. 2014) potentially influencing the carbon cycling of Arctic surface waters at the transition from ice algae to phytoplankton growth periods. Increased organic matter inputs into surface waters will promote bacterial secondary production and release of nutrients, which, coupled with predicted increases in phytoplankton activity (Moreau et al. 2015), will result in overall increases in ecosystem productivity.

Melted out sea ice algal biomass (including the associated dissolved and particulate EPS matrices) is a source of marine aggregates containing significant amounts of Chl *a* and POC (Assmy et al. 2013). The TEP and polysaccharides in the

$pCHO_{HB}$ and $pCHO_{HW}$ and $dEPS_{complex}$ fractions would further contribute to aggregate formation which could result in sea-ice organic carbon reaching deep ocean layers (Riedel et al. 2006; Koch et al. 2014). A deeper flux of sea ice carbon, driven by aggregate-inducing carbohydrates, may also be expected with an earlier onset of ice melt if grazers who feed on the aggregates are not yet present (Carmack and Wassman 2006). In addition, the enrichment of polysaccharides rich in fucose and xylose, such as in sea ice $pCHO_{HB}$ and $pCHO_{HW}$ and $dEPS_{complex}$ contribute to the development of microaggregates at the sea surface microlayer (Russell et al. 2010) which via bubble trapping can become incorporated into atmospherically active aerosols (Leck and Bigg 2010; Leck et al. 2013; Wilson et al. 2015) in the Arctic.

The many roles of sea ice carbohydrates are pertinent at local and regional scales. The existence of relationships between sea ice physical properties, ice algae Chl *a* and dissolved carbohydrate concentrations (Meiners et al. 2012; Underwood et al. 2013), coupled with the characterisation of the complete sea ice carbohydrate budget reported here, provide a basis for modelling sea ice CHO_{TOTAL} at regional scales. Understanding the production and composition of sea ice carbohydrates under future sea ice conditions, and their fate as they are released into the water column, is an important area of future work to understand changes in carbon cycling and microbial activity in the context of rapidly changing Arctic seas.

References

Abdullahi, A. S., G. J. C. Underwood, and M. R. Gretz. 2006. Extracellular matrix assembly in diatoms (Bacillariophyceae). V. Environmental effects on polysaccharide synthesis in the model diatom, *Phaeodactylum tricornutum*. J. Phycol. **42**: 363–378. doi:10.1111/j.1529-8817.2006.00193.x

Amon, R. M., W. H.-P. Fitznar, and R. Benner. 2001. Linkages among the bioreactivity, chemical composition, and diagenetic state of marine dissolved organic matter. Limnol. Oceanogr. **46**: 287–297. doi:10.4319/lo.2001.46.2.0287

Aslam, S. N., T. Cresswell-Maynard, D. N. Thomas, and G. J. C. Underwood. 2012a. Production and characterization of the intra-and extracellular carbohydrates and polymeric substances (EPS) of three sea-ice diatom species, and evidence for a cryoprotective role for EPS. J. Phycol. **48**: 1494–1509. doi:10.1111/jpy.12004

Aslam, S. N., and others. 2012b. Dissolved extracellular polymeric substance (dEPS) dynamics and bacterial growth during sea ice formation in an ice tank study. Polar Biol. **35**: 661–676. doi:10.1007/s00300-011-1112-0

Assmy, P., and others. 2013. Floating ice-algal aggregates below melting Arctic sea ice. PLOS ONE **8**: e7659. doi:10.1371/journal.pone.0076599

Bates, N. R., and J. T. Mathis. 2009. The Arctic Ocean marine carbon cycle: Evaluation of air-sea CO_2 exchanges, ocean

acidification impacts and potential feedbacks. Biogeo-sciences **6**: 2433–2459. doi:10.5194/bg-6-2433-2009

Bellinger, B. J., A. S. Abdullahi, M. R. Gretz, and G. J. C. Underwood. 2005. Biofilm polymers: Relationship between carbohydrate biopolymers from estuarine mud-flats and unialgal cultures of benthic diatoms. Aquat. Microb. Ecol. **38**: 169–180. doi:10.3354/ame038169

Bellinger, B. J., G. J. C. Underwood, S. E. Ziegler, and M. R. Gretz. 2009. Significance of diatom-derived polymers in carbon flow dynamics within estuarine biofilms deter-mined through isotopic enrichment. Aquat. Microb. Ecol. **55**: 169–187. doi:10.3354/ame01287

Belzile, C., S. Brugel, C. Nozais, Y. Gratton, and S. Demers. 2008. Variations of the abundance and nucleic acid con-tent of heterotrophic bacteria in Beaufort Shelf waters during winter and spring. J. Mar. Syst. **74**: 946–956. doi:10.1016/j.jmarsys.2007.12.010

Bitter, T., and H. M. Muir. 1962. A modified uronic acid car-bazole reaction. Anal. Biochem. **4**: 330–334. doi:10.1016/0003-2697(62)90095-7

Bruckner, C. G., C. Rehm, H. P. Grossart, and P. G. Kroth. 2011. Growth and release of extracellular organic com-pounds by benthic diatoms depend on interactions with bacteria. Environ. Microbiol. **13**: 1052–1063. doi:10.1111/j.1462-2920.2010.02411.x

Campbell, K. L., C. J. Mundy, D. G. Barber, and M. Gosselin. 2014. Characterizing the ice algae biomass-snow depth relationship over spring melt using transmitted irradiance. J. Mar. Syst. **147**: 76–84. doi:10.1016/j.jmarsys.2014.01.008

Carmack, E., and P. Wassman. 2006. Food webs and physi-cal–biological coupling on pan-Arctic shelves: Unifying concepts and comprehensive perspectives. Prog. Ocean-ogr. **71**: 446–477. doi:10.1016/j.pocean.2006.10.004

Chin, W. C., M. V. Orellana, and P. Verdugo. 1998. Sponta-neous assembly of marine dissolved organic matter into polymer gels. Nature **391**: 568–572. doi:10.1038/35345

Chiovitti, A., P. Molino, S. A. Crawford, R. W. Teng, T. Spurck, and R. Wetherbee. 2004. The glucans extracted with warm water from diatoms are mainly derived from intracellular chrysolaminaran and not extracellular poly-saccharides. Eur. J. Phycol. **39**: 117–128. doi:10.1080/0967026042000201885

Chiovitti, A., R. E. Harper, A. Willis, A. Bacic, P. Mulvaney, and R. Wetherbee. 2005. Variations in the substituted 3-linked mannans closely associated with the silicified walls of diatoms. J. Phycol. **41**: 1154–1161. doi:10.1111/j.1529-8817.2005.00140.x

Clark, G. F., J. S. Stark, E. L. Johnston, J. W. Runcie, P. M. Goldsworthy, B. Raymond, and M. J. Riddle. 2013. Light-driven tipping points in polar ecosystems. Glob. Chang. Biol. **19**: 3749–3761. doi:10.1111/gcb.12337

Cohen, J., and others. 2014. Recent Arctic amplification and extreme mid-latitude weather. Nat. Geosci. **7**: 627–637. doi:10.1038/ngeo2234

Cota, G. F., and others. 1987. Nutrient fluxes during extended blooms of Arctic ice algae. J. Geophys. Res. **92**: 1951–1962. doi:10.1029/JC092iC02p01951

Decho, A. W. 2000. Microbial biofilms in intertidal systems: An overview. Cont. Shelf Res. **20**: 1257–1273. doi:10.1016/S0278-4343(00)00022-4

Deming, J. W. 2010. Sea ice bacteria and viruses, p. 247–282. *In* D. N. Thomas and G. S. Dieckmann [eds.], Sea ice, 2nd ed. Wiley-Blackwell.

Dubois, M., K. A. Gilles, J. K. Hamilton, P. A. Rebers, and F. Smith. 1956. Colorimetric method for determination of sugars and related substances. Anal. Chem. **28**: 350–356. doi:10.1021/ac60111a017

Dumont, I., V. Schoemann, D. Lannuzel, L. Chou, T-L. Tison, and S. Becquevort. 2009. Distribution and charac-terization of dissolved and particulate organic matter in Antarctic pack ice. Polar Biol. **32**: 733–750. doi:10.1007/s00300-008-0577-y

Ewert, M., and J. W. Deming. 2013. Sea ice microorganisms: Environmental constraints and extracellular responses. Biology **2**: 603–628. doi:10.3390/biology2020603

Fernández-Méndez, M., and others. 2015. Photosynthetic production in the Central Arctic during the record sea-ice minimum in 2012. Biogeosci. Discuss. **12**: 2897–2945. doi:10.5194/bgd-12-29897-2015

Geider, R. J., H. L. MacIntyre, and T. M. Kana. 1998. A dynamic regulatory model of phytoplankton acclimation to light, nutrients and temperature. Limnol. Oceanogr. **43**: 679–694. doi:10.4319/lo.1998.43.4.0679

Giroldo, D., A. A. H. Vieira, and B. S. Paulsen. 2003. Relative increase of deoxy sugars during microbial degradation of an extracellular polysaccharide released by a tropical freshwater *Thalassiosira* sp.(Bacillariophyceae). J. Phycol. **39**: 1109–1115. doi:10.1111/j.0022-3646.2003.03-006.x

Gosselin, M., L. Legendre, J. C. Therriault, S. Demers, and M. Rochet. 1986. Physical control of the horizontal patchi-ness of sea ice microalgae. Mar. Ecol. Prog. Ser. **29**: 289–298. doi:10.3354/meps029289

Granskog, M. A., H. Kaartokallio, H. Kuosa, D. N. Thomas, J. Ehn, and E. Sonninen. 2005. Scales of horizontal patchi-ness in chlorophyll *a*, chemical and physical properties of landfast sea ice in the Gulf of Finland (Baltic Sea). Polar Biol. **28**: 276–283. doi:10.1007/s00300-004-0690-5

Haynes, K., T. A. Hofmann, C. J. Smith, A. S. Ball, G. J. C. Underwood, and A. M. Osborn. 2007. Diatom-derived car-bohydrates as factors affecting bacterial community com-position in estuarine sediments. Appl. Environ. Microbiol. **73**: 6112–6124. doi:10.1128/AEM.00551-07

Herborg, L. M., D. N. Thomas, H. Kennedy, C. Haas, and G. C. Dieckmann. 2001. Dissolved carbohydrates in Antarctic sea ice. Antarct. Sci. **13**: 119–125. doi:10.1017/S0954102001000190

Hezel, P. J., X. Zhang, C. M. Bitz, B. P. Kelly, and F. Massonnet. 2012. Projected decline in spring snow depth

on Arctic sea ice caused by progressively later autumn open ocean freeze-up this century. Geophys. Res. Lett. **39**: L17505. doi:10.1029/2012GL052794

Hoagland, K. D., J. R. Rosowski, M. R. Gretz, and S. C. Roemer. 1993. Diatom extracellular polymeric substances-function, fine structure, chemistry, and physiology. J. Phycol. **29**: 537–566. doi:10.1111/j.0022-3646.1993.00537.x

Hofmann, T., A. R. M. Hanlon, J. D. Taylor, A. S. Ball, A. M. Osborn, and G. J. C. Underwood. 2009. Dynamics and compositional changes in extracellular carbohydrates in estuarine sediments during degradation. Mar. Ecol. Prog. Ser. **379**: 45–58. doi:10.3354/meps07875

Hop, H., S. Falk-Petersen, H. Svendsen, S. Kwasniewski, V. Pavlov, O. Pavlova, and J. E. Søreide. 2006. Physical and biological characteristics of the pelagic system across Fram Strait to Kongsfjorden. Prog. Oceanogr. **71**: 182–231. doi:10.1016/j.pocean.2006.09.007

Juhl, A. R., C. Krembs, and K. M. Meiners. 2011. Seasonal development and differential retention of ice algae and other organic fractions in first year Arctic sea ice. Mar. Ecol. Prog. Ser. **436**: 1–16. doi:10.3354/meps09277

Juul-Pedersen, T., C. Michel, M. Gosselin, and L. Seuthe. 2008. Seasonal changes in the sinking export of particulate material under first-year sea ice on the Mackenzie Shelf (western Canadian Arctic). Mar. Ecol. Prog. Ser. **353**: 13–25. doi:10.3354/meps07165

Kempema, E. W., E. Reimnitz, and P. W. Barnes. 1989. Sea ice sediment entrainment and rafting in the Arctic. J. Sed. Petrol. **59**: 308–317.

Koch, B. P., G. Kattner, M. Witt, and U. Passow. 2014. Molecular insights into the microbial formation of marine dissolved organic matter: Recalcitrant or labile? Biogeosciences **11**: 4173–4190. doi:10.5194/bg-11-4173-2014

Kocum, E., D. B. Nedwell, and G. J. C. Underwood. 2002. Regulation of phytoplankton primary production along a hypernutrified estuary. Mar. Ecol. Prog. Ser. **231**: 13–22. doi:10.3354/meps231013

Krembs, C., H. Eicken, K. Junge, and J. W. Deming. 2002. High concentration of exopolymeric substances in Arctic winter seawater: Implication for the polar ocean carbon cycle and cryoprotection of diatoms. Deep-Sea Res. **49**: 2163–2181. doi:10.1016/S0967-0637(02)00122-X

Krembs, C., and J. W. Deming. 2008. The role of exopolymers in microbial adaptation to sea-ice, p. 247–264. *In* R. Margesin, F. Schinner, J.-C. Marx and C. Gerday [eds.], Psychrophiles: From biodiversity to biotechnology. Springer-Verlag.

Krembs, C., H. Eicken, and J. W. Deming. 2011. Exopolymer alteration of physical properties of sea ice and implications for ice habitability and biogeochemistry in a warmer Arctic. Proc. Natl. Acad. Sci. USA **108**: 3653–3658. doi:10.1073/pnas.1100701108

Lange, B. A., and others. 2015. Comparing springtime ice-algal chlorophyll a and physical properties of multi-year

and first-year sea ice from the Lincoln Sea. PLoS ONE **10**: e0122418. doi:10.1371/journal.pone.0122418

Lavoie, D., K. Denman, and C. Michel. 2005. Modelling ice algae growth and decline in a seasonally ice-covered region of the Arctic Ocean (Resolute Passage, Canadian Archipelago). J. Geophys. Res. **110**: C11009. doi:10.1029/2005JC002922

Leck, C., and E. K. Bigg. 2010. New particle formation of marine biological origin. Aerosol Sci. Technol. **44**: 570–577. doi:10.1080/02786826.2010.481222

Leck, C., Q. Gao, F. M. Rad, and U. Nilsson. 2013. Size-resolved atmospheric particulate polysaccharides in the high summer Arctic. Atmos. Chem. Phys. **13**: 2573–12588. doi:10.5194/acp-13-12573-2013

Liu, S.-B., and others. 2013. Structure and ecological roles of a novel exopolysaccharide from the Arctic sea ice bacterium *Pseudoalteromonas* sp. Strain SM20310. Appl. Environ. Microbiol. **79**: 224–230. doi:10.1128/AEM.01801-12

Mancuso Nichols, C., J. P. Bowman, and J. Guezennec. 2005. Effects of incubation temperature on growth and production of exopolysaccharides by two Antarctic sea ice bacterium grown in batch cultures. Appl. Environ. Microbiol. **71**: 3519–3523. doi:10.1128/AEM.71.7.3519-3523.2005

McConville, M. J. 1985. Chemical composition and biochemistry of sea ice microalgae, p. 105–129. *In* R. A. Horner [ed.], Sea ice biota. CRC Press.

Meiners, K., R. Gradinger, J. Fehling, G. Civitarese, and M. Spindler. 2003. Vertical distribution of exopolymer particles in sea ice of the Fram Strait (Arctic) during autumn. Mar. Ecol. Prog. Ser. **248**: 1–13. doi:10.3354/meps248001

Meiners, K., R. Brinkmeyer, M. A. Granskog, and A. Lindfors. 2004. Abundance, size distribution and bacterial colonization of exopolymer particles in Antarctic sea ice (Bellingshausen Sea). Aquat. Microb. Ecol. **35**: 283–296. doi:10.3354/ame035283

Meiners, K. M., and others. 2012. Chlorophyll *a* in Antarctic sea ice from historical ice core data. Geophys. Res. Lett. **39**: L21602. doi:10.1029/2012GL053478

Michel, C., L. Legendre, R. G. Ingram, M. Gosselin, and M. Levasseur. 1996. Carbon budget of ice algae under first-year ice: Evidence of a significant transfer to zooplankton grazers. J. Geophys. Res. **101**: 18345–18360. doi:10.1029/96JC00045

Michel, C., R. G. Ingram, and L. R. Harris. 2006. Variability in oceanographic and ecological processes in the Canadian Arctic Archipelago. Prog. Oceanogr. **71**: 379–401. doi:10.1016/j.pocean.2006.09.006

Michel, C., and others. 2015. Arctic Ocean outflow shelves in the changing Arctic: A review and perspectives. Prog. Oceanogr. **139**: 66–88. doi:10.1016/j.pocean.2015.08.007

Miller, L. A., and others. 2015. Methods for biogeochemical studies of sea ice: The state of the art, caveats, and recommendations. Elementa Sci. Anthropocene **3**. 000038. doi:10.12952/journal.elementa.000038

Moreau, S., B. Mostajir, S. Bélanger, I. R. Schloss, M. Vancoppenolle, S. Demers, and G. A. Ferreyra. 2015. Climate change enhances primary production in the western Antarctic Peninsula. Glob. Chang. Biol. **21**: 2191–2205. doi:10.1111/gcb.12878

Niemi, A., C. Michel, K. Hille, and M. Poulin. 2011. Protist assemblages in winter sea ice: Setting the stage for the spring ice algal bloom. Polar Biol. **34**: 1803–1817. doi: 10.1007/s00300-011-1059-1

Niemi, A., G. Meisterhans, and C. Michel. 2014. Response of under-ice prokaryotes to experimental sea-ice DOM enrichment. Aquat. Microb. Ecol. **73**: 17–28. doi:10.3354/ame01706

Parsons, T. R., Y. Maita, and C. M. Lalli. 1984. A manual of chemical and biological methods for sea water analysis. Pergamon Press.

Paterson, H., and J. Laybourn-Parry. 2012. Sea ice microbial dynamics over an annual ice cycle in Prydz Bay, Antarctica. Polar Biol. **35**: 993–1002. doi:10.1007/s00300-011-1146-3

Perkins, R. G., G. J. C. Underwood, V. Brotas, G. C. Snow, B. Jesus, and L. Ribeiro. 2001. Responses of microphytobenthos to light: Primary production and carbohydrate allocation over an emersion period. Mar. Ecol. Prog. Ser. **223**: 101–112. doi:10.3354/meps223101

Piwosz, K., J. M. Wiktor, A. Niemi, A. Tatarek, and C. Michel. 2013. Mesoscale distribution and functional diversity of picoeukaryotes in the first-year sea ice of the Canadian Arctic. ISME J. **8**: 1461–147. doi:10.1038/ismej.2013.39

Polyakov, I. V., J. E. Walsh, and R. Kwok. 2012. Recent changes of arctic multiyear sea ice coverage and the likely causes. Bull. Am. Meteorol. Soc. **93**: 145–151. doi: 10.1175/BAMS-D-11-00070.1

Poulin, M., N. Daugbjerg, R. Gradinger, L. Ilyash, T. Ratkova, and C. von Quillfeldt. 2011. The pan Arctic biodiversity of marine pelagic and sea-ice unicellular eukaryotes: A first-attempt assessment. Mar. Biodivers. **41**: 13–28. doi: 10.1007/s12526-010-0058-8

Poulin, M., G. J. C. Underwood, and C. Michel. 2014. Sub-ice colonial *Melosira arctica* in Arctic first-year ice. Diatom Res. **29**: 213–221. doi:10.1080/0269249X.2013.877085

Poulsen, N., N. Kroger, M. J. Harrington, E. Brunner, S. Paasch, and M. T. Buhmann. 2014. Isolation and biochemical characterization of underwater adhesives from diatoms. Biofouling **30**: 513–523. doi:10.1080/08927014.2014.895895

Riedel, A., C. Michel, M. Poulin, and S. Lessard. 2003. Taxonomy and abundance of micro algae and protists at a first-year sea ice station near Resolute Bay, Nunavut, spring to early summer 2001. Canadian Data Report of. Hydrographic and Ocean Sciences, 159, vi + 53 p.

Riedel, A., C. Michel, and M. Gosselin. 2006. Seasonal study of sea-ice exopolymeric substances on the Mackenzie shelf: Implications for transport of sea-ice bacteria and algae. Aquat. Microb. Ecol. **45**: 195–206. doi:10.3354/ame045195

Riedel, A., C. Michel, M. Gosselin, and B. LeBlanc. 2007. Enrichment of nutrients, exopolymeric substances and microorganisms in newly formed sea ice on the Mackenzie shelf. Mar. Ecol. Prog. Ser. **342**: 55–67. doi:10.3354/meps342055

Russell, L. M., L. N. Hawkins, A. A. Frossard, P. K. Quinn, and T. S. Bates. 2010. Carbohydrate-like composition of submicron atmospheric particles and their production from ocean bubble bursting. Proc. Natl. Acad. Sci. USA **107**: 6652–6657. doi:10.1073/pnas.0908905107

Rysgaard, S., M. Kuhl, R. N. Glud, and H. J. Würgler. 2001. Biomass, production and horizontal patchiness of sea ice algae in a high-Arctic fjord (Young Sound, NE Greenland). Mar. Ecol. Prog. Ser. **223**: 15–26.

Smith, R. E. H., J. R. Cavaletto, B. J. Eadie, and W. S. Gardner. 1993. Growth and lipid composition of high Arctic ice algae during the spring bloom at Resolute, Northwest Territories, Canada. Mar. Ecol. Prog. Ser. **97**: 19–29. doi:10.3354/meps097019

Stedmon, C. A., D. N. Thomas, M. Granskog, H. Kaartokallio, S. Papadimitriou, and H. Kuosa. 2007. Characteristics of dissolved organic matter in Baltic coastal sea ice: Allochthonous or autochthonous origins? Environ. Sci. Technol. **41**: 7273–7279. doi:10.1021/es071210f

Steele, D. J., D. J. Franklin, and G. J. C. Underwood. 2014. Protection of cells from salinity stress by extracellular polymeric substances in diatom biofilms. Biofouling **30**: 987–998. doi:10.1080/08927014.2014.960859

Stroeve, J. C., M. C. Serreze, M. M. Holland, J. E. Kay, J. Malanik, and A. P. Barrett. 2012. The Arctic's rapidly shrinking sea ice cover: A research synthesis. Clim. Change **110**: 1005–1027. doi:10.1007/s10584-011-0101-1

Stroeve, J. C., T. Markus, L. Boisvert, J. Miller, and A. Barrett. 2014. Changes in Arctic melt season and implications for sea ice loss. Geophys. Res. Lett. **41**: 1216–1225. doi: 10.1002/2013GL058951

Sutherland, I. 2001. Biofilm exopolysaccharides: A strong and sticky framework. Microbiology **147**: 3–9. doi:10.1099/00221287-147-1-3

Swart, N. C., J. C. Fyfe, E. Hawkins, J. E. Kay, and A. Jahn. 2015. Influence of internal variability on Arctic sea-ice trends. Nat. Clim. Change **5**: 86–89. doi:10.1038/nclimate2483

Thomas, D. N., S. Papadimitriou, and C. Michel. 2010. Biogeochemistry of sea ice, p. 425–468. *In* D. N. Thomas and G. S. Dieckmann [eds.], Sea ice, 2nd ed. Wiley-Blackwell.

Tremblay, G., C. Belzile, M. Gosselin, M. Poulin, S. Roy, and J.-É. Tremblay. 2009. Late summer phytoplankton distribution along a 3500 km transect in Canadian Arctic waters: Strong numerical dominance by picoeukaryotes. Aquat. Microb. Ecol. **54**: 55–70. doi:10.3354/ame01257

Underwood, G. J. C., and D. M. Paterson. 2003. The importance of extracellular carbohydrate production by marine epipelic diatoms. Adv. Bot. Res. **40**: 184–240. doi:10.1016/S0065-2296(05)40005-1

Underwood, G. J. C., M. Boulcott, C. A. Raines, and K. Waldron. 2004. Environmental effects on exopolymer production by marine benthic diatoms: Dynamics, changes in composition, and pathways of production. J. Phycol. **40**: 293–304. doi:10.1111/j.1529-8817.2004.03076.x

Underwood, G. J. C., S. Fietz, S. Papadimitriou, D. N. Thomas, and G. S. Dieckmann. 2010. Distribution and composition of dissolved extracellular polymeric substances (EPS) in Antarctic sea ice. Mar. Ecol. Prog. Ser. **404**: 1–19. doi:10.3354/meps08557

Underwood, G. J. C., and others. 2013. Broad-scale predictability of carbohydrates and exopolymers in Antarctic and Arctic sea ice. Proc. Natl. Acad. Sci. USA **110**: 15734–15739. doi:10.1073/pnas.1302870110

van der Merwe, P., and others. 2009. Biogeochemical observations during the winter-spring transition in East Antarctic sea ice: Evidence of iron and exopolysaccharide controls. Mar. Chem. **115**: 163–175. doi:10.1016/j.marchem.2009.08.001

Vancoppenolle, M., and others. 2013. Role of sea ice in global biogeochemical cycles: Emerging views and challenges. Quat. Sci. Rev. **79**: 207–230. doi:10.1016/j.quascirev.2013.04.011

Verdugo, P. 2012. Marine microgels. Ann. Rev. Mar. Sci. **4**: 375–400. doi:10.1146/annurev-marine-120709-142759

Werner, I., J. Ikävalko, and H. Schünemann. 2007. Sea-ice algae in Arctic pack ice during late winter. Polar Biol. **30**: 1493–1504. doi:10.1007/s00300-007-0310-2

Wilson, T. W., and others. 2015. A marine biogenic source of atmospheric ice-nucleating particles. Nature **525**: 234–238. doi:10.1038/nature14986

Wustman, B. A., M. R. Gretz, and K. D. Hoagland. 1997. Extracellular matrix assembly in diatoms (Bacillariophyceae) I. A model of adhesives based on chemical characterization and localization of polysaccharides from the marine diatom *Achnanthes longipes* and other diatoms. Plant Physiol. **113**: 1059–1069. doi:10.1104/pp.113.4.1059

Zhou, J., K. Mopper, and U. Passow. 1998. The role of surface active carbohydrates in the formation of transparent exopolymer particles by bubble adsorption of seawater. Limnol. Oceanogr. **43**: 1860–1871. doi:10.4319/lo.1998.43.8.1860